Multimodal brain and retinal imaging of dopaminergic degeneration in Parkinson disease

Jee-Young Lee[1,2]✉, *Antonio Martin-Bastida*[3], *Ane Murueta-Goyena*[4], *Iñigo Gabilondo*[4,5], *Nicolás Cuenca*[6], *Paola Piccini*[7] *and Beomseok Jeon*[1,8]

Abstract | Parkinson disease (PD) is a progressive disorder characterized by dopaminergic neurodegeneration in the brain. The development of parkinsonism is preceded by a long prodromal phase, and >50% of dopaminergic neurons can be lost from the substantia nigra by the time of the initial diagnosis. Therefore, validation of in vivo imaging biomarkers for early diagnosis and monitoring of disease progression is essential for future therapeutic developments. PET and single-photon emission CT targeting the presynaptic terminals of dopaminergic neurons can be used for early diagnosis by detecting axonal degeneration in the striatum. However, these techniques poorly differentiate atypical parkinsonian syndromes from PD, and their availability is limited in clinical settings. Advanced MRI in which pathological changes in the substantia nigra are visualized with diffusion, iron-sensitive susceptibility and neuromelanin-sensitive sequences potentially represents a more accessible imaging tool. Although these techniques can visualize the classic degenerative changes in PD, they might be insufficient for phenotyping or prognostication of heterogeneous aspects of PD resulting from extranigral pathologies. The retina is an emerging imaging target owing to its pathological involvement early in PD, which correlates with brain pathology. Retinal optical coherence tomography (OCT) is a non-invasive technique to visualize structural changes in the retina. Progressive parafoveal thinning and fovea avascular zone remodelling, as revealed by OCT, provide potential biomarkers for early diagnosis and prognostication in PD. As we discuss in this Review, multimodal imaging of the substantia nigra and retina is a promising tool to aid diagnosis and management of PD.

Lewy bodies
Eosinophilic intracytoplasmic neuronal inclusions, composed largely of α-synuclein, that are characteristically found in the brain of individuals with neurodegenerative diseases such as Parkinson disease and dementia with Lewy bodies.

Nigrosomes
Clusters of calbindin-negative dopaminergic cells in the substantia nigra.

✉*e-mail:* wieber04@snu.ac.kr

https://doi.org/10.1038/s41582-022-00618-9

Parkinson disease (PD) is a progressive neurodegenerative disorder that presents clinically with parkinsonism, the cardinal features of which include bradykinesia, rigidity, rest tremor and postural instability. The main pathological hallmarks of brain degeneration in PD are Lewy bodies and neuronal loss. The parkinsonism in patients with PD reflects pathology in the substantia nigra and dysfunction of the nigrostriatal dopaminergic system. However, the condition is associated with a range of additional motor and non-motor features, and the Lewy body pathology extends widely to nervous system structures both within and beyond the CNS, including the enteric plexus, autonomic ganglia, salivary glands, olfactory bulb, retina and skin. Various theories, including Braak's hypothesis on the pathological staging of PD[1], have been put forward to explain how pathology propagates in PD, and this topic remains a matter for debate[2,3]. However, dopaminergic degeneration in the substantia nigra is generally agreed to be the essential pathological feature in PD[4], and detection of early-phase changes in this region is a key target of imaging biomarker development.

In recent years, we have seen considerable advances in MRI techniques for the early detection of dopaminergic degeneration, capturing microstructural changes relating to neurodegeneration, iron accumulation, disappearance of neuromelanin and loss of nigrosomes in the substantia nigra pars compacta (SNc) (FIG. 1). Emerging research is focusing on new MRI techniques to monitor disease progression and multimodal imaging approaches to differentiate atypical parkinsonian syndromes from PD. Owing to the superior accessibility and convenience of MRI compared with techniques such as PET and single-photon emission CT (SPECT), MRI markers for PD are an attractive proposition. However, the new MRI techniques only visualize nigral degeneration and, therefore, might be insufficient for phenotyping or prognostication of heterogeneous aspects of PD that result from extranigral pathologies.

Key points

- Advanced nigral MRI techniques in Parkinson disease (PD) include diffusion tensor free water measurement, quantitative susceptibility mapping of iron signals, evaluation of nigrosome 1 (N1) loss on iron-sensitive sequences and quantification of neuromelanin loss on neuromelanin-sensitive sequences.
- N1 signal loss and neuromelanin reduction in the substantia nigra pars compacta can be detected in prodromal PD, although longitudinal studies are required to validate this approach.
- Multimodal imaging capturing pathological changes in the substantia nigra should substantially enhance diagnostic accuracy in early PD, and longitudinal multimodal MRI studies could provide essential pathophysiological insights and provide markers to monitor disease progression.
- Visual disturbances observed in patients with PD are linked to retinal dopamine loss, which results in functional derangement of couplings between retinal cells and defective synaptic transmission.
- Parafoveal inner retinal change can be detected from the early stages of PD, extending to the macula and peripapillary nerve fibre layer at advanced stages and showing associations with visual hallucinations and cognitive impairment.
- Retinal imaging could provide a convenient imaging tool for early diagnosis and monitoring progression in PD, and further investigation of the link between retinal and brain pathology could provide further pathophysiological insights into neurodegenerative diseases.

To help overcome these limitations, the retina could be a future target of imaging in PD. Owing to its direct connection to the brain and the fact that it can be non-invasively visualized, this structure can provide an important window to brain pathology[5,6]. The retina contains dopaminergic cells, and profound dopamine loss, relating to visual dysfunction, has been observed in the retina in patients with PD[7–12]. Pathological studies have shown a correlation between retinal and brain α-synuclein pathologies in PD[13], and the retina is being used increasingly to investigate PD pathogenesis[14,15]. Optical coherence tomography (OCT) enables histological sections of the retina to be visualized non-invasively in minutes without the need for premedication. OCT studies have shown focal and diffuse retinal changes through various stages of PD, and some promising results have been obtained with regard to early diagnosis and prognostication in PD[11,16–20]. Future imaging techniques in which the resolution is enhanced to the cellular level should improve the detection of dopaminergic cell loss and early morphological changes in retinal ganglion cells (RGCs).

In this article, we review advances in MRI biomarker development for early diagnosis and progression monitoring in PD, with a particular focus on new techniques with longitudinal evidence and applications in prodromal PD, as well as future multimodal approaches. We also review the development of retinal imaging markers for diagnosis and progression of PD and their contribution to understanding the pathophysiology of the condition. After considering the strengths and limitations of the various imaging modalities, we propose the combined application of non-invasive substantia nigra and retinal imaging techniques for future biomarker development in PD.

Author addresses

[1]Department of Neurology, Seoul National University College of Medicine, Seoul, South Korea.
[2]Seoul Metropolitan Government–Seoul National University Boramae Medical Center, Seoul, South Korea.
[3]Department of Neurology and Neurosciences, Clinica Universidad de Navarra, Pamplona–Madrid, Spain.
[4]Neurodegenerative Diseases Group, Biocruces Bizkaia Health Research Institute, Barakaldo, Bizkaia, Spain.
[5]Ikerbasque: The Basque Foundation for Science, Bilbao, Spain.
[6]Department of Physiology, Genetics and Microbiology, University of Alicante, Alicante, Spain.
[7]Division of Neurology, Department of Brain Science, Imperial College London, London, UK.
[8]Seoul National University Hospital, Seoul, South Korea.

Current diagnostic approach to PD

Currently, diagnosis of PD is primarily based on clinical symptoms. The first step is to document parkinsonism via neurological examination, and the second step is to determine whether the parkinsonism is attributable to PD[21]. The presence of bradykinesia, plus rest tremor and/or rigidity, is required for documentation of parkinsonism. In addition, a clinically established PD diagnosis should meet all the following three criteria: first, absence of absolute exclusion criteria; second, at least two supportive criteria; and third, no 'red flag' signs[21]. These three criteria are designed to differentiate PD from atypical parkinsonian syndromes and secondary parkinsonian disorders, such as drug-induced, toxic–metabolic or vascular parkinsonism. Atypical parkinsonian syndromes are neurodegenerative disorders that can present with parkinsonism but have different pathologies and aetiologies from PD. Multiple system atrophy (MSA), progressive supranuclear palsy (PSP) and corticobasal degeneration are the most common disorders in this category. From a clinical perspective, differential diagnosis at the early stages of these disorders is challenging, and because the treatment response and prognosis are generally poor in atypical parkinsonian syndromes compared with PD, development of specific diagnostic markers has been an important priority in neuroimaging research.

Although the diagnosis of PD remains clinically based, neuroimaging tools were incorporated into the recently proposed Movement Disorder Society PD (MDS-PD) diagnostic criteria[21]. Specifically, abnormal denervation on ^{123}I-metaiodobenzylguanidine (^{123}I-MIBG) cardiac scintigraphy was included in 'supportive criteria', and a normal or preserved presynaptic dopaminergic system (as visualized by PET or SPECT, for example) was included in 'absolute exclusion criteria'. In clinical practice, conventional MRI is often performed to exclude structural lesions such as subdural haemorrhage or other space-occupying lesions, normal-pressure hydrocephalus or severe white matter changes that can be linked to the patient's symptoms. However, the resolution of conventional MRI is insufficient to discern changes in the substantia nigra that distinguish people with PD from healthy individuals.

Nuclear imaging of nigrostriatal dopaminergic nerve fibres via PET or SPECT has been available for clinical and research purposes for some time. Typical tracer targets include L-aromatic acid decarboxylase, which converts levodopa to dopamine and can be detected by ^{18}F-dopa; dopamine transporters (DATs) that are exclusively expressed in presynaptic dopaminergic nerve terminals; and synaptic vesicles that are present in

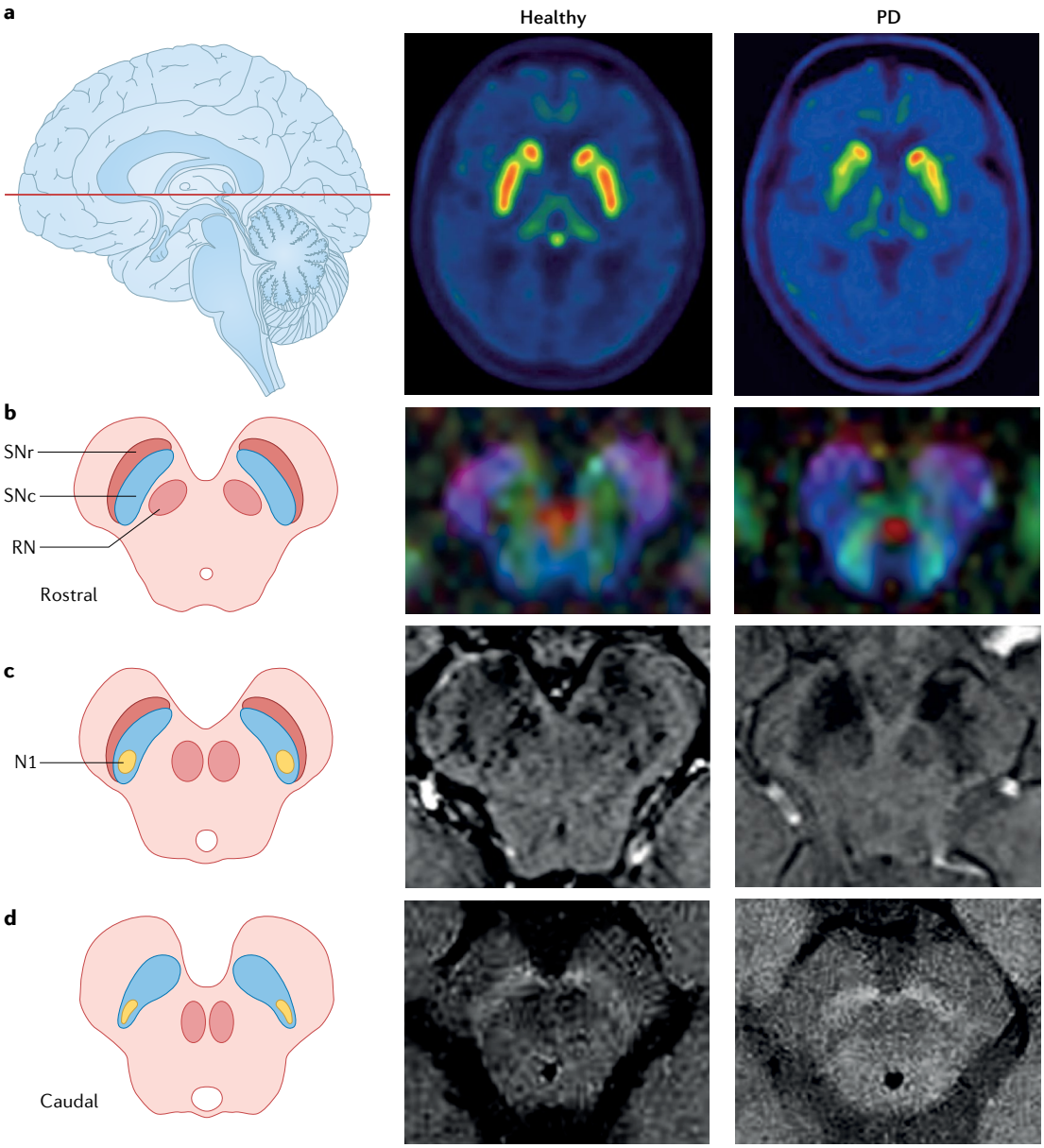

Fig. 1 | **Imaging of microstructural changes in the substantia nigra in PD. a** | At the level of the striatum (line in left-hand image), ^{18}F-fluorodopa PET or dopamine transporter (DAT) PET or single-photon emission CT (SPECT) imaging can be used to assess the integrity of dopaminergic fibre terminals. DAT PET images show bilateral symmetrical uptake of the tracer ^{11}C-PE2I in the striatum, which is reduced in Parkinson disease (PD). **b–d** | The left-hand images illustrate mid-brain slices through the substantia nigra, subdivided into the substantia nigra pars compacta (SNc) and substantia nigra pars reticulata (SNr) with the neighbouring red nucleus (RN). The position of nigrosome 1 (N1) is shown in yellow. The other images show the use of nigral imaging techniques in the brain of healthy individuals and patients with PD. These techniques include fractional anisotropy to analyse the microstructure (part **b**), susceptibility-weighted imaging to visualize iron deposition (part **c**) and T1-weighted fast spin-echo imaging to visualize neuromelanin (part **d**). Patients with PD can show a decrease in fractional anisotropy in the posterior substantia nigra (part **b**) and loss of nigral dorsolateral hyperintensity (part **c**), which reflects N1 signal loss, either unilaterally or bilaterally. The loss of N1 signal spreads to dorsal and medial nigrosomes in association with loss of neuromelanin load, as detected by a reduction in the bright signal volumes of neuromelanin (part **d**) and increased iron deposition (increased hyposignal intensity as in part **c**).

monoaminergic nerve fibres. Among these targets, DAT imaging is the most used modality and has been approved for clinical practice in many European, American and Asian countries. According to the MDS-PD diagnostic criteria[21], preservation of the nigrostriatal dopaminergic system, as revealed by PET or SPECT, is highly diagnostic for exclusion of PD. However, presynaptic dopaminergic PET and SPECT images cannot precisely differentiate atypical parkinsonism from PD, and tracer uptake can be affected by compensatory synaptic plastic changes or by medications that interfere with dopaminergic and other monoaminergic systems. These factors should be considered when using PET or SPECT to monitor disease progression. Furthermore, SPECT has limited resolution,

Melanophagia
Phagocytosis of melanin.

Neuronophagia
Destruction of neurons by phagocytic cells.

Marinesco bodies
Intranuclear inclusions found in pigmented neurons in the substantia nigra.

Somatodendrite
Region of a neuron that includes the cell body and dendrite.

Single-shell scans
Diffusion signal scans acquired in a single shell.

Multi-shell scans
Diffusion signal scans acquired from a multi-shell scheme.

Free water fractional volume
The volume fraction of free water within the regional volume defined by a voxel.

Bi-tensor modelling
A diffusion tensor imaging analysis model consisting of two tensor compartments; for example, free water and tissue compartments.

Fractional anisotropy
A measure of the degree of anisotropy of water molecules in diffusion tensor imaging analysis, which ranges from 0 (infinite isotropy, no restrictions in all directions) to 1 (anisotropy, movement in only one axis and limited to others).

Hoehn and Yahr stages
Clinical staging system for parkinsonian disorders proposed by M. Hoehn and Y. Yahr in 1967.

and PET and SPECT scan cameras and radiotracers are not readily available. In addition, both techniques carry potential radiation risks and are expensive, especially when repeated scans are required to monitor disease progression.

Substantia nigra pathology in PD

The anatomy of the human substantia nigra[22–25] is summarized in BOX 1. Substantia nigra pathology in PD is characterized by neuronal loss in the SNc, particularly the ventrolateral and caudal tiers, which is comparable to dorsal tier neuronal loss during normal ageing[26,27]. Dopaminergic neurons have characteristic pigmented neuromelanin granules that attract metal ions. The substantia nigra is rich in iron, most of which is stored in neuromelanin. Under pathological conditions, iron accumulation increases and the pigmented neurons become depigmented and depleted in number, accompanied by an increase in extracellular neuromelanin levels, along with melanophagia and neuronophagia[28]. Tyrosine hydroxylase-negative melanized SNc neurons with Marinesco bodies in the nucleus can also be detected[29]. In addition, staining for α-synuclein reveals various forms of Lewy pathology, including intracytoplasmic inclusion Lewy bodies, Lewy neurites and pale bodies within the neuromelanin[30], somatodendrite staining, cell soma punctate staining and multilobular Lewy bodies.

Visualizing dopaminergic degeneration by MRI

Diffusion-weighted imaging

The main advantage of diffusion MRI is the ability to quantify microstructural changes in subcortical structures at the voxel level via widely available single-shell scans. Multi-shell scans might also be useful for determining neurite density and configuration — for example, bending or fanning — although this approach is not yet fully established. Diffusion tensor imaging (DTI) studies have produced conflicting results[31]; however, a longitudinal increase in aberrant diffusion signals has been consistently observed in the posterior part of the substantia nigra in people with PD[32,33].

Free water fractional volume estimation through bi-tensor modelling[34] can detect pathological change in the posterior substantia nigra more sensitively than can conventional fractional anisotropy, even after free water correction. Free water fractional volume did not correlate with parkinsonian motor symptoms and putaminal DAT at baseline in two independent early-stage PD cohorts[35], but on follow-up, the free water fraction increased significantly compared with free water-corrected fractional anisotropy or diffusivity values[36]. The free water increase in the posterior substantia nigra correlated with striatal DAT change and increasing Hoehn and Yahr stages over a 4-year follow-up period[37]. A study published in 2021 found a free water increase in the posterior substantia nigra in patients with idiopathic REM sleep behaviour disorder (iRBD), both at baseline and after 18 months' follow-up. Interestingly, the authors found an inverse relationship between free water and putaminal DAT values in these patients[38]. However, in studies conducted in patients with 'moderate'-stage PD, a free water increase was observed in the anterior but not the posterior substantia nigra[39], and neither the longitudinal increase in the substantia nigra free water fraction nor any correlation with clinical symptom progression was replicated in a 2-year follow-up analysis[40]. Therefore, the use of free water measurements to monitor disease progression in early-stage PD might not be generalizable to patients with more advanced PD. Free water estimation might aid the differentiation of atypical parkinsonian syndromes from PD[41], in view of the more widespread pathology and related microstructural changes in the former conditions[42].

Multi-shell diffusion imaging is thought to reflect microstructural changes more precisely than single-shell images, and to be able to estimate partial volume from the cerebrospinal fluid. To date, only three studies have applied multi-shell neurite orientation dispersion and density imaging to PD[43–45]. One of these studies revealed that multi-shell free water imaging was no better than single-shell imaging for differentiating atypical parkinsonian syndromes from PD[45].

In a study reported in 2019, an approach termed automated imaging differentiation of parkinsonism (AID-P), which combines automated analysis with machine learning, was developed with the aim of differentiating atypical parkinsonian syndromes from PD[46]. AID-P was applied to free water fractional volumes and free water-corrected fractional anisotropy measures of 17 subcortical regions and 43 DTI fibre tract images obtained from 1,000 participants from seven centres. This machine-learning approach was found to be feasible for multicentre MRI analysis with discrepant image sequences or scanners and showed good outcomes for differentiating various forms of parkinsonism. AID-P correctly classified five autopsy-confirmed cases of atypical parkinsonism. However, its diagnostic performance in terms of differentiating individuals with early-stage PD from healthy controls was found to be suboptimal and it is unlikely to supersede conventional clinical assessment using the MDS Unified PD Rating Scale (MDS-UPDRS) at present.

Iron-sensitive susceptibility imaging

Iron accumulation in the substantia nigra — and to a lesser extent the globus pallidus and motor cortex — is one of the main pathological hallmarks of PD[47,48]. The increased iron deposition is associated with increased

Box 1 | **Anatomy of the substantia nigra**

The substantia nigra has two anatomically distinct areas: the pars reticulata (SNr) and the pars compacta (SNc). The SNr is the ventral part of the substantia nigra and is mainly composed of GABAergic neurons, whereas the SNc is the dorsal part and comprises dopaminergic neurons. In the human substantia nigra, the boundary between the SNr and SNc is diffuse, and the SNc dopaminergic cells extend in a finger-like fashion into the SNr. Around 60% of the dopaminergic neurons in the SNc are sparsely located in the calbindin-rich zone (matrix), and 40% are packed in the five calbindin-poor zones (nigrosome)[10]. Among the five nigrosomes, nigrosome 1, which is located in the SNc at intermediate and caudal levels, is the largest[11]. Note that calbindin is a marker of striatonigral projection terminals targeting SNr neurons, and the ventral tier of the SNc is mostly devoid of calbindin. The mesencephalic dopaminergic neuronal groups[8] are composed of the SNc cell group (nucleus A9), the retrorubral area cell group (A8), the ventral tegmental area cell group (A10) and the substantia nigra pars dorsalis cell group. The ventral tier of the SNc includes the A9 cell group and the dorsal tier includes A8, A9, A10 and substantia nigra pars dorsalis cells[9].

Partial volume
The actual volume occupied by a small species of molecules or particles in a solution.

Region of interest (ROI) analysis
Analysis of data extracted from specified ROIs for the study.

Quantitative susceptibility mapping
(QSM). An MRI technique for quantifying the spatial distribution of magnetic susceptibility within the tissue.

T2* dephasing
Immediately after forming transverse magnetization by a radiofrequency pulse, the transverse magnetization starts decreasing in magnitude as protons start going out of phase (dephasing). Dephasing can be altered by magnetic field inhomogeneity, magnetic susceptibility difference of various elements in the tissues, and the gradients applied. T2* relaxation is the decay of transverse magnetization with gradient echo sequences, which is used to visualize haemorrhage, calcification and iron deposition.

Fast spin-echo
An MRI technique that records multiple echoes after a 90° excitation pulse by transmitting a series of 180° inversion pulses at set intervals. By contrast, the conventional spin-echo sequence measures a single echo.

Magnetization transfer
The transfer of nuclear spin polarization and/or coherence from one population of nuclei to another. This technique can suppress background signals to improve contrast on MRI scans.

levels of ferritin, which could potentially influence the MRI contrast owing to its superparamagnetic properties[49].

Iron-sensitive MRI techniques, such as relaxometry (T2* or R2*) and susceptibility-weighted imaging (SWI), revealed increased nigral iron accumulation in PD, which was associated with disease severity in most studies[50]. However, the sensitivity and specificity of the techniques were variable, and heterogeneous results were obtained in extra-nigral deep nuclei. A meta-analysis of 11 post-mortem and 33 MRI studies in people with PD concluded that relaxometry and SWI techniques could authentically reflect iron changes in the substantia nigra but not in other subcortical nuclei[51]. Increased nigral iron deposition can be detected in individuals with prodromal PD manifestations, such as iRBD, and the deposition increases further as the disease progresses[52].

Of note, substantia nigra region of interest (ROI) analysis based on susceptibility or relaxometry maps has been suggested to produce inconsistent results[53], and studies in both cross-sectional[54] and longitudinal cohorts[55] have indicated that a neuromelanin image-driven ROI approach can provide more robust diagnostic value with regard to ventrolateral substantia nigra iron accumulation in PD. Quantitative susceptibility mapping (QSM) can also improve the accuracy of iron measurement, and has been shown to pinpoint iron accumulation specifically in the SNc[56]. QSM can also be used to investigate the pattern of whole-brain iron accumulation in PD[57] and has demonstrated associations between cognitive dysfunction and cortical and striatal iron accumulation[58]. The longitudinal studies that have measured iron accumulation in PD[55,59,60] are summarized in Supplementary Tables 1 and 2.

Loss of dorsolateral hyperintensity of the substantia nigra on susceptibility imaging is another potential marker of PD. This so-called swallow tail sign[61] is comparable to the pathological pattern of nigrosome loss that has been observed in post-mortem studies of individuals with PD[24,25]. Of the five nigrosomes that have been observed in the brain, nigrosome 1 (N1) shows the earliest and most explicit involvement in PD and produces the highest diagnostic yield on 7 T MRI experiments[62,63]. Loss of N1 at early stages of PD is also known to be associated with increased iron accumulation[61]. Therefore, imaging techniques that employ dorsolateral nigral hyperintensity (DNH) as a marker for nigrosome loss could aid the early diagnosis of PD. In support of this proposal, the incidence of DNH loss in iRBD cohorts (50–78%) is higher than in control groups (<20%) but lower than in PD groups (79–90%)[64,65]. In patients with iRBD, N1 signal loss detected on 3 T MRI showed 63% concordance with DAT reduction in iRBD, increasing to 87% with 7 T MRI[66]. Therefore, detection of N1 loss via DNH change is a promising diagnostic MRI marker of nigral degeneration that could be applied in the prodromal stages of PD. However, the diagnostic value of N1 signal loss for differentiating atypical parkinsonian syndromes from PD was found to be poor[67,68].

With the current technology, identification of N1 through DNH imaging is subjective and depends on the scanning protocol and imaging sequences. The diagnostic sensitivity and specificity reported in patients with early-stage PD was generally >80%, but some studies reported much lower sensitivities. Implementation of QSM in imaging protocols[69–72] and modification of the scan protocol (for example, by analysing the lower part of the substantia nigra border, which shows low susceptibility signals, and making the imaging plane perpendicular to the axis of N1) could improve the diagnostic accuracy[73]. However, high iron content can lead to T2* dephasing at the edge of the substantia nigra, thereby producing a false N1 signal[71]. Currently, we lack a standard quantification method for N1 loss and no correlation of this MRI marker with disease severity has been detected, thereby challenging its use for monitoring disease progression. A study published in 2020, which applied a semiquantitative measure of nigrosome intensity, showed that DNH loss was a gradual phenomenon during the transition from the healthy state thorough iRBD to PD[74]. To fully realize the potential of N1 loss as a marker for PD, large-scale and long-term follow-up studies should be conducted, in addition to establishing standard imaging techniques[75].

Neuromelanin-sensitive imaging

Neuromelanin is a dark complex pigment that is found in dopaminergic neurons of the SNc and the ventral tegmental area and noradrenergic neurons of the locus coeruleus. Intracellular neuromelanin resides in double-membraned autophagic neuromelanin organelles that reside in the cytoplasm, distant from the nucleus[76]. Neuromelanin is generated through catecholaminergic metabolism of dopamine and norepinephrine. Excess cytosolic catecholamines that are not incorporated into synaptic vesicles undergo iron-mediated oxidation, after which they react with β-sheet proteins to form neuromelanin[77]. Neuromelanin displays strong affinities for metals such as iron (in the iron-rich SNc) and copper (in the copper-rich locus coeruleus). Under normal conditions, iron is sequestered and maintained in the redox-inactive form, so neuromelanin acts as a chelator of redox-active metals[78]. However, under oxidative conditions such as in PD, iron is sequestered in its redox-active form, thereby promoting deleterious oxidative stress through redox reactions. Extracellularly released metals from neuromelanin could potentially activate microglia, leading to release of pro-inflammatory cytokines, increased oxidative stress, neurodegeneration and accumulation of α-synuclein[79].

The neuromelanin–iron complex is paramagnetic, causing an increase in the T1 signal on MRI[80]. High-resolution T1-weighted imaging with fast spin-echo and magnetization transfer pulses has been used to visualize neuromelanin in the midbrain and other pigmented nuclei[81]. Reductions in nigral neuromelanin volume or contrast are a common finding in neuromelanin-sensitive MRI studies of individuals with PD[82–84]. However, this technique has only 60–80% sensitivity for differentiating people with PD from healthy controls, which is no better than DAT imaging. The reductions in neuromelanin volume in the substantia nigra were found to be more severe in the lateral (or posterior) part of this brain region and in patients with longer disease durations[84,85].

Area under the curve (AUC). Area under the receiver operating characteristic curve (integral) ranging from 0 (no discriminative ability) to 1 (the highest-level ability) to evaluate an ability of a classifier under a classification threshold.

Results pertaining to locus coeruleus depigmentation are more heterogeneous[83,86,87], possibly owing to variations in analytical methods, including the number of brain slices analysed and ROI delineation on individual slices. Such variations might have led to underestimation of neuromelanin loss in the locus coeruleus. Nevertheless, neuromelanin loss in the locus coeruleus, in addition to the SNc, was shown to have good discriminative value for distinguishing MSA parkinsonism from other parkinsonian disorders, including PD (60% sensitivity and 90% specificity) and PSP syndrome (80% sensitivity and 85% specificity)[87,88].

As an alternative to manual analysis, voxel-wise analysis using a normalized neuromelanin MRI template from healthy controls could improve the quantification of neuromelanin. This approach showed a gradient of neuromelanin volume loss in patients with PD, with the most severe loss in the posterior SNc followed by the anterior SNc and the locus coeruleus[89]. A good correlation was observed between normalized neuromelanin volume loss and parkinsonian symptom severity, as assessed by the UPDRS[89], although the effects of levodopa medication on this MRI marker were not fully examined. Voxel-wise assessment of neuromelanin volume loss in the substantia nigra revealed exponential decay of nigral neuromelanin, which, on the basis of extrapolation of the decay curve, was suggested to start ~5.3 years before a clinical PD diagnosis[90]. This study also showed that the clinical association of nigral neuromelanin loss paralleled the pattern of functional organization of motor, cognitive and behavioural loops throughout the nigrostriatal system[90], consistent with histological and post-mortem studies. Longitudinal studies that measured neuromelanin volume reduction and contrast ratios in the substantia nigra[90–92] are summarized in Supplementary Tables 1 and 2.

Interestingly, neuromelanin loss in the locus coeruleus was found to be more severe in PD patients with polysomnography-confirmed RBD than in those without RBD, and also correlated with abnormally increased muscle tone during REM sleep[93]. In a subsequent study, neuromelanin loss in the locus coeruleus had >80% sensitivity and specificity for differentiating patients with iRBD from healthy controls[94]. A multimodal imaging study showed locus coeruleus neuromelanin reduction in patients with iRBD who had no striatal dopamine depletion[95]. Therefore, in synucleinopathies, neuromelanin loss in the locus coeruleus might be an earlier pathological event than dopaminergic loss. Neuromelanin loss in the SNc was also found in another iRBD cohort[96]. Therefore, evaluation of neuromelanin intensity in the SNc and locus coeruleus is a promising imaging tool, although robust longitudinal and multi-platform studies of neuromelanin-sensitive MRI in the prodromal stage and early-stage PD populations will be needed to test its validity for diagnosing PD and monitoring disease progression.

Multimodal MRI applications

Neuromelanin-sensitive imaging of the SNc has been shown to improve the diagnostic value and robustness of other nigral imaging techniques, such as DTI and iron-sensitive imaging, in PD. DTI of an ROI defined by neuromelanin-sensitive MRI showed significant fractional anisotropy reduction and diffusivity increase in the ventrolateral SNc in patients with PD compared with controls, whereas the same DTI analysis performed on a T2-derived ROI showed negative results[97,98]. Another study applied a single seven-echo 3D SWI sequence with a magnetization transfer contrast pulse to simultaneously evaluate iron and neuromelanin in the SNc in 40 patients with early-stage PD and 40 controls[99]. Of the various individual measures, neuromelanin volume had the highest diagnostic value (area under the curve (AUC) 0.960), although the substantia nigra iron content (AUC 0.740) or iron volume (AUC 0.788) or the N1 sign (AUC 0.891) could increase the diagnostic performance to AUC >0.960 if combined with neuromelanin volume[99]. Simultaneous analysis of multiple MRI parameters in the substantia nigra can also provide complementary information regarding nigral degeneration in early-stage PD[99]. With a total scanning time of <5 min to generate 64 slices, this single-sequence scan approach is also attractive from a practical perspective.

Multimodal MRI of the SNc is also useful for studying prodromal PD[96]. When used in combination, neuromelanin volume (AUC 0.85) and signal loss (AUC 0.82) and fractional anisotropy measurements on a neuromelanin-derived SNc ROI (AUC 0.77) allowed the detection of nigral degeneration in patients with iRBD with good diagnostic accuracy (AUC 0.95), whereas diffusivity measures or iron quantification showed no discriminative value.

Interestingly, both N1 imaging and neuromelanin-sensitive MRI have been shown to aid the differentiation of tremor-dominant PD from essential tremor[100,101], and the combination of both imaging techniques greatly improved the diagnostic performance (AUC >0.93)[102].

On the basis of multimodal MRI studies so far, neuromelanin-sensitive imaging seems to be the most efficient MRI marker of PD and might be useful in the prodromal phase. However, further investigation via multimodal and combined MRI techniques is required to specify the sequence of early pathological signals in the substantia nigra and to visualize progression of those pathological changes in PD. Machine-learning analysis of variables obtained from multimodal MRI might further enhance the diagnostic value of iron-sensitive and neuromelanin-sensitive imaging in parkinsonian disorders.

Multimodal MRI and DAT imaging

Levels of presynaptic dopaminergic markers have been shown to decrease exponentially in patients with PD, possibly beginning up to 10 years before the clinical appearance of parkinsonism[103]. In patients with early-onset PD (<44 years of age), the presynaptic dopaminergic fibre density was lower at the time of symptom onset and the subsequent decay was slower than in individuals with late-onset PD (>66 years of age)[104]. Through backwards extrapolation of the decay curves, the authors concluded that the presymptomatic phase spans more than two decades in patients with early-onset PD, compared with one decade in those with late-onset PD.

These results suggest that DAT imaging can be used to monitor disease progression in asymptomatic individuals with any degree of DAT loss, and that individuals with PD onset at a relatively young age might benefit the most from future neuroprotective therapeutics. Currently, DAT imaging is the only validated imaging tool to monitor disease progression in prodromal and early-stage PD. The annual DAT reduction rate in the striatum is reported to be 5–6% in individuals with iRBD[105,106] and 4–5% in those with early-stage PD[103,107]. In addition, DAT imaging can provide risk stratification in the population of individuals with prodromal PD[105,108,109] and could be used to select potential participants for clinical trials investigating neuroprotective or disease-modifying therapeutics.

Few studies have directly compared nigral MRI techniques with DAT imaging in PD, although some important correlations and discordances have been observed. One longitudinal study in a cohort of individuals with early-stage PD showed that the posterior substantia nigra free water measure did not significantly correlate with putaminal DAT levels at baseline; however, over a 4-year follow-up period, an increase in free water was paralleled by a decline in putaminal DAT[35,37]. The free water increase was most rapid during the first 2 years. The authors calculated that the required sample sizes for potential neuroprotective clinical trials based on free water estimation are comparable to those based on DAT SPECT, and could be even smaller if the target population is confined to those with newly diagnosed early-stage PD[37]. Another study found that DTI measures correlate poorly with dopaminergic degeneration, as measured by DAT and D2 receptor SPECT, in people with PD[110].

Several studies have addressed the longitudinal trajectory of longitudinal neuromelanin loss in relation to DAT in PD. In two studies that used neuromelanin-sensitive MRI and ^{123}I-FP-CIT SPECT, substantia nigra neuromelanin volumes and substantia nigra and locus coeruleus contrast ratios correlated with putaminal DAT in individuals with PD[111,112]. The asymmetry indices of neuromelanin loss and DAT loss also correlated with one another, but substantia nigra neuromelanin volumes showed weaker correlations with the UPDRS score than did DAT levels[112]. Another study analysed ventral and dorsal SNc neuromelanin contrast ratios and the corresponding nigral, putamen and caudate DAT levels, as measured using ^{11}C-PE2I PET, in the most and least affected sides in 30 patients with moderate-stage PD[113]. The neuromelanin contrast ratio reduction was more severe in the ventral SNc than in the dorsal SNc, and a notable left–right asymmetry was found in both SNc neuromelanin and DAT, although the asymmetry was much less marked than for striatal DAT. Furthermore, a discrepancy was observed between the clinical laterality and reductions in the nigral neuromelanin and DAT levels. By contrast, striatal DAT showed a good correlation with clinical laterality in PD. The possibility of underestimation of neuromelanin cannot be excluded in this study, but no clear relationship was found between SNc neuromelanin contrast reduction and nigral DAT loss, although significant correlations were detected between neuromelanin loss and striatal DAT reductions. The SNc neuromelanin contrast ratio correlated with disease duration but not with the motor UPDRS score, whereas DATs did correlate with this score.

The discrepancies in clinical laterality support previous observations that striatal DAT is related to the degree of axonal damage and shows a floor effect when nigral cell loss reaches ≥50%[114,115]. Striatal DAT is closely related to striatal dopamine levels, which might explain its correlation with clinical symptoms, whereas nigral DAT is more likely to reflect the nigral cell count[114]. On the other hand, the discrepancy between neuromelanin loss and SNc DAT might reflect different aspects of neurodegeneration in PD. One study investigated the relationship between melanized neuron and tyrosine hydroxylase-positive (TH^+) dopaminergic neuron loss in post-mortem brains from patients with varying PD durations[116]. Loss of melanized neurons was found to lag behind the loss of dopamine markers and was slow and variable in the early years of PD, whereas TH^+ neuronal loss and putaminal loss of dopaminergic markers occurred rapidly within the first few years. In a recent multicentre longitudinal study, neuromelanin-sensitive and iron-sensitive nigral MRI and striatal DAT SPECT scans were performed in 135 patients with early-stage PD, 43 patients with iRBD and 55 healthy controls[117]. Around half of the participants received 2-year follow-up scans. By extrapolating from the baseline and follow-up data, the researchers estimated the trajectory of decay of imaging markers and proposed that striatal DAT levels started to decrease at ~13 years and neuromelanin loss began at 4–5 years before clinical PD diagnosis, although considerable interindividual variability was observed. Both the striatal DAT and the nigral neuromelanin reductions were detected first in sensorimotor areas, followed by cognitive and limbic areas in that order. However, QSM analysis for nigral iron did not recapitulate this pattern, suggesting that increases in iron levels do not always correlate with pathological processes in the substantia nigra.

Future perspectives for brain imaging

Multimodal approaches that combine nigral MRI and dopaminergic imaging will need to be tested in a large prospective cohort to ascertain the validity of MRI markers for detecting prodromal PD and predicting subsequent disease conversion, monitoring PD progression and monitoring the effects of neuroprotective and neurorestorative therapeutics such as cell transplantation, gene therapy, immunotherapy and iron chelation therapy. Investigation of nigral MRI techniques in conjunction with imaging or body fluid markers of neuroinflammation (astrocyte-associated or microglia-associated) and misfolded α-synuclein is also warranted. This multimodal analytical approach could potentially enhance both the diagnostic and pathophysiological value of nigral MRI. In addition, MRI protocols for capturing the N1 signal or neuromelanin loss need to be optimized to increase reproducibility and signal-to-noise ratios.

Scotopic and photopic b-waves
Short flashes can elicit an electroretinogram consisting of initial negative deflection (a-wave) and a following positive deflection (b-wave). The b-waves in response to scotopic and photopic stimuli reflect rod and cone ON bipolar cell depolarization, respectively.

Because PD has extranigral pathologies, multimodal imaging that evaluates both nigral and extranigral (non-dopaminergic) pathologies might enable phenotyping and prognostication of heterogeneous clinical features in PD. One study evaluated intestinal parasympathetic cholinergic denervation by ^{11}C-donepezil PET–CT, cardiac sympathetic denervation by ^{123}I-MIBG scintigraphy, neuromelanin loss and noradrenergic denervation in the locus coeruleus by neuromelanin-sensitive MRI and ^{11}C-methylreboxetine PET, and nigrostriatal dopaminergic degeneration by ^{18}F-DOPA PET in patients with iRBD or PD[2]. The study provided valuable insights into pathological progression in PD, including evidence for brain-first and body-first subtypes. However, this multimodal imaging approach is impractical for clinical use owing to its high cost and inaccessibility.

Retinal imaging

Although the newer MRI techniques have advantages over conventional MRI and PET and SPECT, visualization of neurodegeneration in the substantia nigra has limitations, and the MRI signal changes might not accurately reflect neuronal loss. Retinal imaging is an emerging imaging modality that has the potential to reflect brain pathology as well as PD-related retinal degeneration.

Retinal dysfunction and pathology in PD

The characteristics of retinal dysfunction in PD are listed in BOX 2. In 1990, Harnois and Di Paolo described a decrease in dopamine levels in post-mortem retinal tissue from patients with PD[7]. Profound dopamine loss in the retina has also been detected in neurotoxin-based animal models of PD[118–120]. The retinal dopaminergic cells reside at the border of the inner plexiform and inner nuclear layers and they release dopamine in a circadian manner[8,121]. The roles of dopamine in the retinal synapses and intercellular coupling[8,121,122] are described in FIG. 2.

The first evidence of visual pathway impairment in PD, manifesting as abnormal visual evoked potentials, was published in 1978 (REF.[123]). A subsequent electroretinography study published in 1987 showed specific impairment of RGC function in patients with PD[124], and later studies confirmed this finding[125–129]. PD-associated attenuation of electrical signals in the retina could be reversed by levodopa administration[9,124,130], indicating a dopaminergic influence on RGC activities. Dopamine modulates the crosstalk between different retinal circuits and optimizes the signal-to-noise ratio, thereby tuning the spatial contrast responses of the retina. Pattern electroretinography experiments in primates using dopamine D1 and D2 receptor antagonists and a D1 receptor agonist showed that different types of dopamine receptors are involved in retinal contrast tuning[131]. Patients with PD have attenuated responses to both high-frequency and low-frequency contrasts, although high frequencies are preferentially affected. The attenuated response was most prominent in the 'off'-medication condition in patients with PD and motor fluctuations[9], and was improved by levodopa medication[10,132]. The contrast sensitivity defect was also identified in patients with iRBD[122]. The contrast impairment points towards foveal dysfunction and dopaminergic defects impairing horizontal cell coupling in PD[12,133].

At least 43 prospective studies have shown objective impairment of visual afferent function in patients with PD, with consistent reports of decline in contrast sensitivity and altered colour discrimination[123,132,134–155]. Reductions in high-contrast visual acuity have also been described in PD[156,157], although low-contrast visual acuity seems to be preferentially affected[16,157–159]. Eye movements have a crucial role in contrast detection and visual scenery screening, and disturbances in saccades and smooth pursuit[160,161], which can be partially restored with dopaminergic therapy[160,162,163], could contribute to visual defects in patients with PD. Alterations in superior colliculus-mediated functional activities have been found in patients with de novo PD and might be attributable to defective retinal signals or brainstem pathology[164]. Clinically, visual complaints such as blurring, dimness, poor contrast, double vision and minor illusory symptoms are frequent in PD[165,166], and some patients have even stated that their visual symptoms preceded the motor symptoms[167]. Patients with PD also have reduced visuospatial abilities[16,166,168–170], possibly owing to visual afferent dysfunction, although top-down control could produce the same symptoms.

Evidence suggests that the retina in patients with PD reflects brain pathology. In healthy individuals, α-synuclein is expressed abundantly in the retinal pigment epithelium (RPE) and neural retinal cells, including amacrine and bipolar cells. Despite some methodological difficulties in studying α-synuclein in the retina[171],

Box 2 | **Retinal dysfunction in Parkinson disease**

Functional changes
- Contrast sensitivity impairment (especially at high spatial frequencies).
- Impairment in colour discrimination.
- Intermittent double vision.
- Decreased visual acuity (under high-contrast and low-contrast conditions).
- Reduced scotopic and photopic b-waves on electroretinography.

Structural changes
- Thinning of the inner retina, especially at the parafovea.
- Parafoveal ganglion cell–inner plexiform layer thinning correlates with nigral dopamine loss
- Remodelling of foveal avascular zone.
- Progressive thinning of the macular inner retinal layers and peripapillary retinal nerve fibre layers over time.

Pathological changes
- Dopaminergic amacrine cell loss with a gradient from the parafoveal to the perifoveal region and less in the periphery of the retina.
- Abnormal coupling of horizontal, amacrine and ganglion cells owing to reduced dopamine levels.
- Reduced density of photosensitive melanopsin-containing retinal ganglion cells and loss of dopaminergic synaptic contacts to these cells.
- Possible circadian dysregulation resulting from disruption of the retinal melanopsin system.
- Phosphorylated α-synuclein aggregates resembling Lewy bodies and Lewy neurites in ganglion cell bodies and dendrites.

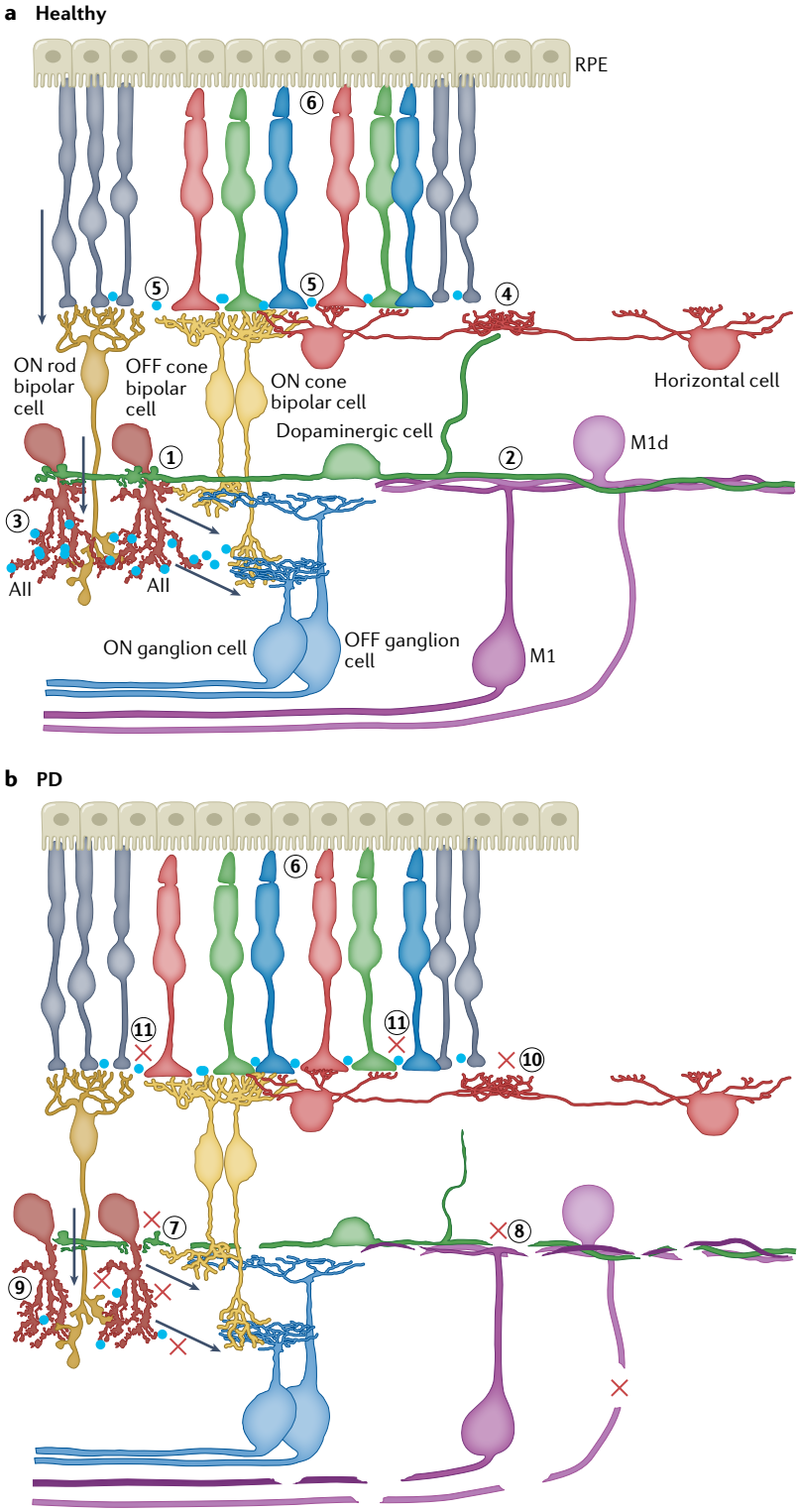

Fig. 2 | **Retinal changes in PD. a** | Structure and circuitry of the healthy retina. Dopaminergic cells make synaptic contacts with AII amacrine and melanopsin-photosensitive ganglion cells in the inner plexiform layer. Dopamine uncouples the gap junctions between photoreceptors, horizontal cells and AII-type amacrine cells. Arrows indicate transmission of information in the scotopic pathway. The rod signal is transmitted to ON rod bipolar cells that contact the AII amacrine cells. These amacrine cells transfer information to OFF cone bipolar cells through chemical synapses and to ON cone bipolar cells via gap junctions, incorporating the rod signal to the cone pathway. **b** | The retina in Parkinson disease (PD), showing death of dopaminergic cells and loss of their synaptic contacts with AII amacrine cells and melanopsin retinal ganglion cells (M-RGCs). Loss of connexin 36 is also observed, reflecting defective cell–cell coupling through gap junctions. M-RGCs (melanopsin 1 (M1) and melanopsin 1 displaced (M1d)) constitute ~0.2% of the total RGC population and have important roles in non-image-forming functions, such as light entrainment of circadian rhythms, sleep-onset modulation and melatonin suppression. These cells also participate in non-image-forming functions that interact with the image-forming process, including pupillary light responses and mediation of signals to the superior colliculus and lateral geniculate nucleus[168]. The number of M-RGCs normally falls after the age of 70 years, accompanied by age-dependent atrophy of dendritic arborization[170], and the reduction in M-RGC density is even greater in people with PD[171]. The intrinsically photosensitive M-RGCs receive dopaminergic input, and daytime release of dopamine is counteracted by melatonin release at night. Thus, an intact retinal melanopsin system is necessary to maintain circadian rhythms. Dopamine loss results in persistent coupling of photoreceptor, horizontal and amacrine cells, and defective dopaminergic synapses affect synaptic transmission in the scotopic pathway and melanopsin system. These alterations could explain the visual dysfunction and the circadian rhythm and sleep disturbances that are observed in PD[169]. RPE, retinal pigment epithelium.

researchers were able to demonstrate aggregation of abnormally phosphorylated (pSer129) α-synuclein (p-αSC) in post-mortem retinal tissue samples from patients with PD[13,172], especially in the RGC complexes. Morphological changes and p-αSC aggregates within the RGCs resembled degenerating neurons of the brain, and Lewy neurite-like structures were also found in the PD retina[13]. Interestingly the burden of retinal α-synucleinopathy correlated with premorbid parkinsonian symptom severity and brain α-synucleinopathy[13]. Retinal Lewy pathology has also been reported in incidental Lewy body disease[13] — that is, Lewy pathology in the absence of parkinsonian symptoms — suggesting the possibility of retinal involvement in prodromal PD (FIG. 3). Retinal α-synucleinopathy could be useful for studying the neuropathological mechanisms underlying PD, and retinal p-αSC might be a biomarker of PD.

Ortuño-Lizarán et al. found degeneration of dopaminergic cells and their dendritic plexus in post-mortem retinal tissue from people with PD[12]. The authors summarized the main retinal features in PD as loss of dopaminergic synaptic contacts with AII amacrine cells (as also observed in a primate model of PD)[173] and a decrease in gap junction connections (connexin 36)[174]

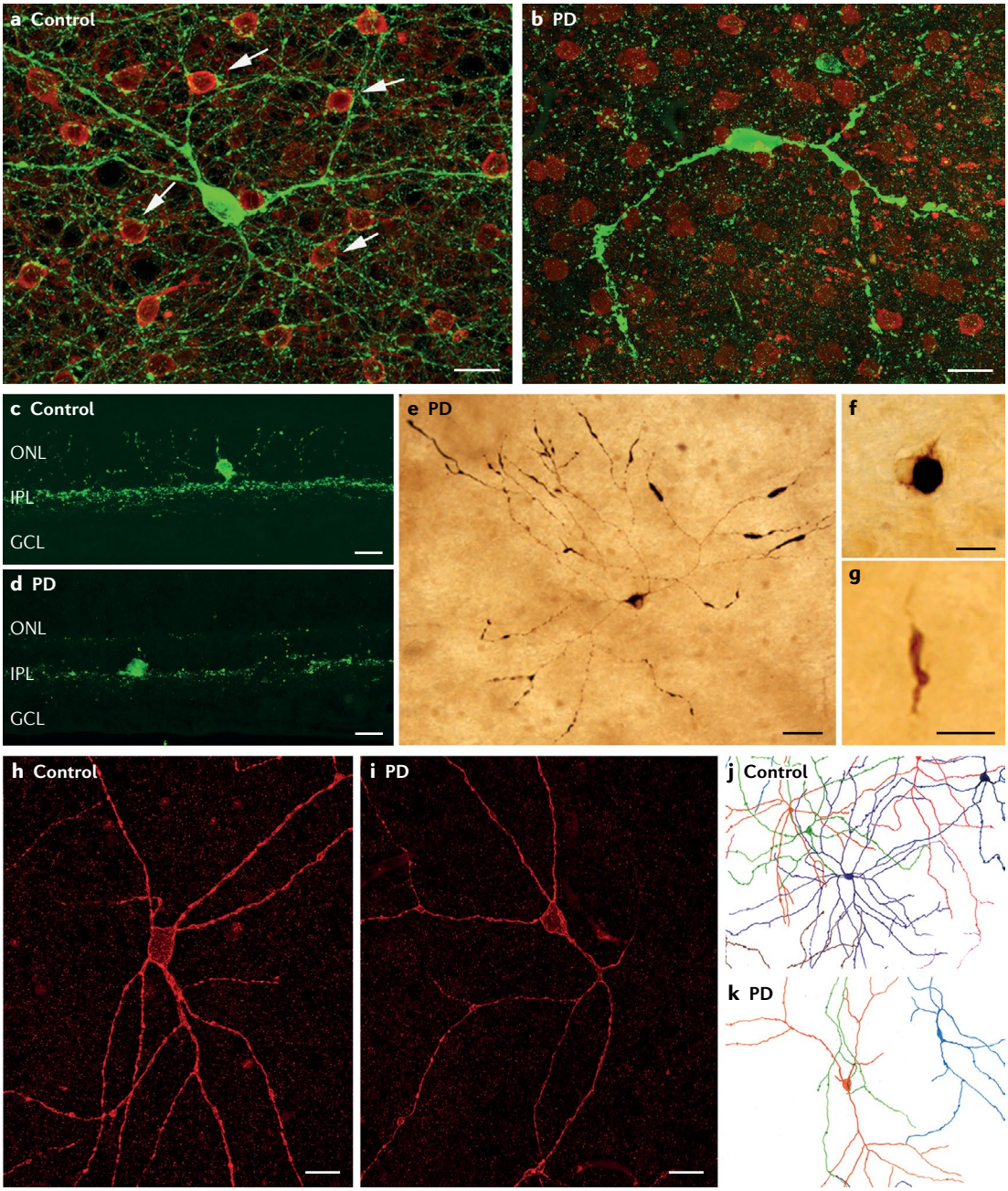

between AII amacrine cells[12] (FIGS 2,3). The association between dopamine loss and synaptic deafferentation of melanopsin RGCs provides a pathophysiological clue to visual dysfunction as well as circadian rhythm disorders observed in patients with PD[175–178] (FIG. 2).

Renewal of photoreceptor outer segments and phagocytosis by the RPE is important for maintaining normal vision. This process involves assembly of photoreceptor disc membranes, disc shedding (controlled by an intrinsic circadian oscillator, which uses dopamine and melatonin as light and dark signals, respectively) and phagocytosis of the discs by the RPE[179]. During phagocytosis, iron-rich ferritin can be released from RPE cells[14]. Accumulation of α-synuclein in the RPE impairs ferritinophagy, especially after high-intensity light exposure, and when α-synuclein-overexpressing RPE cells are exposed to excess iron, both α-synuclein and ferritin are released from cells in exosomes[14], thereby raising the possibility of α-synuclein spreading in the retina, as is observed in the brain. Experiments in the TgM83 transgenic mouse model of α-synucleinopathy showed that intracerebral inoculation of brain homogenate from old and clinically ill TgM83 mice accelerated abnormal p-αSC accumulation, microglial activation and dysregulation of macroautophagy in the retinas of young mice[15]. Therefore, by providing a window into the brain, retinal imaging might aid pathophysiological research and therapeutic development in PD.

Optical interferometry
A measurement method using the phenomenon of interference of light waves. Medical imaging using low-coherence interferometry can provide tomographic visualization of internal tissue microstructure.

Retinal optical coherence tomography

General principles. OCT is a non-invasive, high-resolution in vivo imaging technique based on the optical interferometry principle and can provide rapid and highly reproducible 3D structural images of the retina[180] (FIG. 4).

◀ Fig. 3 | **Visualizing retinal pathology in PD. a**,**b** | Wholemount retinal preparations double immunostained with antibodies against tyrosine hydroxylase (green) and calretinin (red) — markers for dopaminergic neurons and AII amacrine cells, respectively. In the healthy retina (part **a**), the long, thin dendrites of dopaminergic neurons form a dense plexus with ringed structures contacting AII amacrine cell bodies (arrows). In Parkinson disease (PD) (part **b**), swelling of dendrites and loss of the dopaminergic plexus and the rings surrounding AII amacrine cells are observed. **c**,**d** | Cross-sectional views of the dopaminergic plexus in stratum S1 of the inner plexiform layer (IPL) and their projections from dopaminergic neurons to the outer nuclear layer (ONL). This plexus appears as a continuous dense and complex structure in the healthy retina (part **c**) and is markedly reduced in PD (part **d**). **e**–**g** | Retinal tissue in PD, immunostained with antibodies against Ser129-phosphorylated α-synuclein. Part **e** shows a ganglion cell with phosphorylated α-synuclein aggregates in the cell body and dendrites. Parts **f** and **g** show a Lewy body and Lewy neurite-like structures, respectively. **h**,**i** | Melanopsin cells visualized by immunohistochemistry with antibodies against melanopsin. Part **h** shows typical melanopsin cell morphology with numerous dendritic branches and long dendrites, which form a complex plexus in the IPL. In PD (part **i**), fewer dendritic branches and thinner dendrites are observed. **j**,**k** | Camera lucida drawings showing reductions in the complexity of the melanopsin plexus and melanopsin cell density in PD compared with controls. Scale bars: parts **a**–**d**, **f**, **h** and **i**, 20 mm; part **e**, 50 mm; part **g**, 10 mm. GCL, ganglion cell layer. Parts **e**,**f** and **g** reprinted with permission from REF.[13], Wiley.

OCT can detect and quantify retinal alterations that could be biomarkers for brain diseases[5,181]. Advantages of OCT include good accessibility in hospitals with ophthalmology departments, low cost compared with MRI in most countries, lack of radiation hazard, and no requirement for premedication. However, image acquisition can be hampered by ophthalmological comorbidities that are common in the ageing population, such as severe cataracts, glaucoma and retinal vessel or macular diseases.

Despite high accuracy and precision, commercially available OCT devices vary in acquisition speed and depth resolution, as well as in scanning protocols, acquisition parameters and built-in segmentation algorithms. Therefore, OCT measurements are not directly comparable between different commercial devices. Furthermore, no consensus exists on the PD diagnostic protocol; for example, which retinal areas or subsectors should be included in thickness calculations and which statistical methods should be used to correct for the effects of multiple comparisons within and between individuals. Consequently, the retinal OCT research community has developed the Advised Protocol for OCT Study Terminology and Elements (APOSTEL) initiative (BOX 3) to provide recommendations for analysing and reporting OCT data in neurological disorders[182,183].

Retinal nerve fibre layer and macular thinning. Several studies have used OCT to evaluate peripapillary retinal nerve fibre layer (pRNFL) thickness in PD, with contradictory results. Some authors have found significant thinning of the pRNFL in people with PD compared with controls[23,125,184–200], but around one-third of studies failed to find such differences[17,136,201–211]. Similarly, measurements of macular volume and thickness in PD have yielded conflicting results, although thinning of the inner retinal layers, in particular the ganglion cell–inner plexiform layer (GCIPL), is a consistent observation, providing robust evidence of selective retinal atrophy[16–19,189,197,202,206,212–216]. A meta-analysis concluded that patients with PD exhibit thinning of pRNFL and inner retinal layers with relatively spared outer retinal layers[217].

At least 20 cross-sectional studies have evaluated the correlation between pRNFL or macular measurements and disease duration, with variable results[17,23,184–195,198,199,201,203,205–207,210,211] (Supplementary Table 3). The link with motor severity is also uncertain, with some studies showing a clear correlation with pRNFL[187,188,190,192,213] or macular thickness[19,184,192,205,209,215,218,219] and others indicating no such relationship[141,185,186,193,195,197,199,201,203,206,211,220–222]. As regards non-motor aspects of PD, some cross-sectional studies have revealed that macular thinning is related to worse outcomes on visual parameters, such as low-contrast visual acuity, contrast sensitivity, colour vision or visual cognition[16,141,223]. Also, a relationship between visual hallucinations and macular inner layer thinning has been observed[17,218]. The few studies that have explored the association between retinal parameters and mild cognitive changes are more consistent, showing decreased cognitive abilities in patients with PD who have reduced pRNFL[196,197,200,224] and macular thickness, especially in the GCIPL[18,20].

As patients with PD are often in the honeymoon phase of dopaminergic treatment, the true disease severity is difficult to determine on the basis of UPDRS scores in the medication 'on' state. Therefore, the correlations reported in OCT studies need to be interpreted with caution if the medication condition is not specified. In addition, many cross-sectional studies had small sample sizes and did not consider ophthalmological comorbidities or other factors that could affect retinal thickness, such as age, axial length of individual eyes and intra-individual interocular differences.

On the basis of OCT studies in PD to date, pRNFL or macular atrophy seems to be more evident in more advanced stages of the disease, although in early stages focal thinning can be detected in the inner retinal layers of the macula, mainly in the parafoveal area (FIG. 5; Supplementary Table 3). The clinical implications of retinal atrophy need further investigation, using longitudinal data with sufficiently long-term follow-up periods. Interestingly, some studies suggest that retinal involvement is an early event with variable progression depending on the clinical subtype of PD[16,20,198,211]. Observations of OCT alterations in patients with iRBD[11], who are at high risk of developing the predominant postural instability–gait disorder — or 'body-first' — phenotype of PD[2], and increased retinal impairment in aggressive PD caused by the autosomal dominant E46K mutation in the α-synuclein (*SNCA*) gene[16] further corroborate the idea of early retinal impairment in certain clinical subtypes of PD[11,20].

Parafoveal thinning. Early electrophysiological studies and clinical symptoms observed in patients with PD suggested that dysfunction of the central macula — that is, the fovea — is a distinctive feature of the disease. In humans, dopaminergic projections innervate the cells within the foveal avascular zone (FAZ)[225], and dopamine loss in the degenerating retina is a key event for visual defects, as it alters the crosstalk between horizontal cells,

Peripapillary retinal nerve fibre layer
(pRNFL). Retinal nerve fibre layer bundle that passes through the optic papilla (optic disc).

Honeymoon phase
A period of relative stability with an excellent response to levodopa in patients with Parkinson disease, which usually lasts for a few years following the start of levodopa therapy.

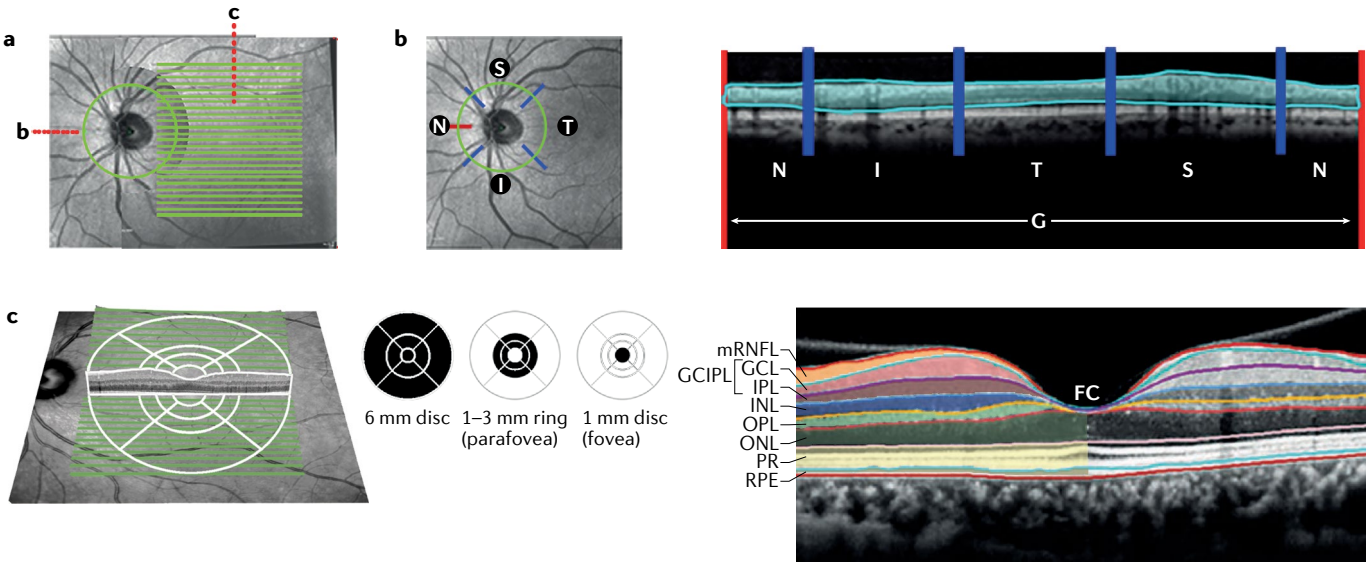

Fig. 4 | **Acquisition and analysis of retinal OCT images.** Retinal optical coherence tomography (OCT; part **a**) provides peripapillary circular images (part **b**) and images with multiple parallel linear slices (raster scans) of the macula (part **c**). Owing to the well-structured anatomy of the retina, OCT allows different cell layers of the macula and the peripapillary nerve fibre layer (pRNFL) to be discerned. The built-in software of modern OCT devices can automatically delimit or segment the edges of retinal layers and quantify point-by-point thicknesses and mean thicknesses of different regions of interest. In peripapillary circular images (part **b**), the software automatically segments the pRNFL and provides the mean global pRNFL thickness (G) by averaging the thickness of the four main radial sectors — temporal (T), nasal (N), superior (S) and inferior (I) — in a circular section (green line) with a diameter of 3.0–4.5 mm around the optic disc. In macular raster-scan images (part **c**), the software segments the main layers and layer complexes of the retina; that is, the macular retinal nerve fibre layer (mRNFL), the ganglion cell–inner plexiform layer (GCIPL) complex, the inner nuclear layer (INL), the complex formed by the outer plexiform, Henle's fibre and outer nuclear layers (OPL–HF–ONL) and external limiting membrane–Bruch's membrane (ELM–BM), or segments the seven retinal layers separately (mRNFL, ganglion cell layer (GCL), inner plexiform layer (IPL), INL, OPL, ONL and photoreceptors–retinal pigment epithelium (PR–RPE)). Typically, OCT studies report average macular thickness or volume measurements in Early Treatment Diabetic Retinopathy Study maps, which consist of a standardized circular grid centred on the fovea composed of a central 1-mm circle and two concentric 3-mm and 6-mm diameter rings divided into four radial sectors of 90° (T, N, S and I), thereby dividing the macula into nine subsectors. FC, fovea centralis.

AII amacrine cells and ganglion cell connections[226], which can precede photoreceptor cell damage[227]. These findings justify investigation of the fovea and parafoveal region in patients with PD.

Only a few studies have specifically investigated parafoveal thickness in patients with PD by modifying the conventional OCT grid[16,19,228]. The parafovea is the circular area, ~2.5–3.0 mm in diameter, around the centre of the fovea. The peak RGC density (35,100 cells per mm^2) is found ~1 mm from the centre of the fovea (circle 2 mm in diameter), and most RGCs reside within the circle ~3.5–4.0 mm in diameter[229]. Parafoveal thinning is a relatively focal structural change and can only be detected by OCT using a contracted small-diameter circular window. The currently available built-in OCT software provides automatic thickness measurement in a 6 mm diameter grid, and the inclusion of unaffected or less affected areas within the measurement window can lead to underestimation of parafoveal thinning.

Using a 1/2.25/3.41 mm diameter modified Early Treatment of Diabetic Retinopathy Study circle to analyse OCT scans from drug-naive patients with PD, Ahn et al. investigated the relationship between parafoveal inner retinal layer thinning and dopaminergic loss in the brain, as measured using ^{18}F-FP-CIT PET[19]. In these patients, GCIPL thinning in the parafovea correlated with DAT reduction in the substantia nigra[19], with the inferior and temporal sectors of the parafovea being the most affected areas[19,230]. These findings are in line with the results of a neuropathological study showing the topography of retinal dopamine loss in retinal tissue from patients with PD[12]. In addition, GCIPL thickness in the parafoveal inferior and temporal sectors in patients with iRBD was found to be in the intermediate range between controls and patients with de novo PD, correlating with olfactory impairment and striatal DAT reductions[11,230]. These findings suggest that parafoveal thinning could be a marker of prodromal Lewy body disease.

Another study regionalized macular OCT scan images into various concentric circles and rings to analyse the specific topographical changes in the macula of patients with PD, using retinal measurements from patients with aggressive Lewy body diseases — that is, dementia with Lewy bodies and PD caused by the E46K

Box 3 | **The APOSTEL recommendation for OCT studies**

In the original Advised Protocol for OCT Study Terminology and Elements (APOSTEL) recommendations[177], a panel of experienced optical coherence tomography (OCT) researchers (11 neurologists, two ophthalmologists and two neuroscientists) created a list of recommendations for reporting quantitative OCT studies, including study protocol, acquisition device and settings, scanning protocol, details of funduscopic imaging, post-acquisition data selection and image processing, and statistical analyses, as well as stating which anatomical retinal regions and layers should be analysed. Although this guideline was originally developed for retinal OCT studies in multiple sclerosis, it can be directly applied to OCT studies in PD. An update of the APOSTEL criteria was published in 2021 and included suggestions from 116 authors of articles in which retinal OCT was applied to various ophthalmological and neurological conditions[178].

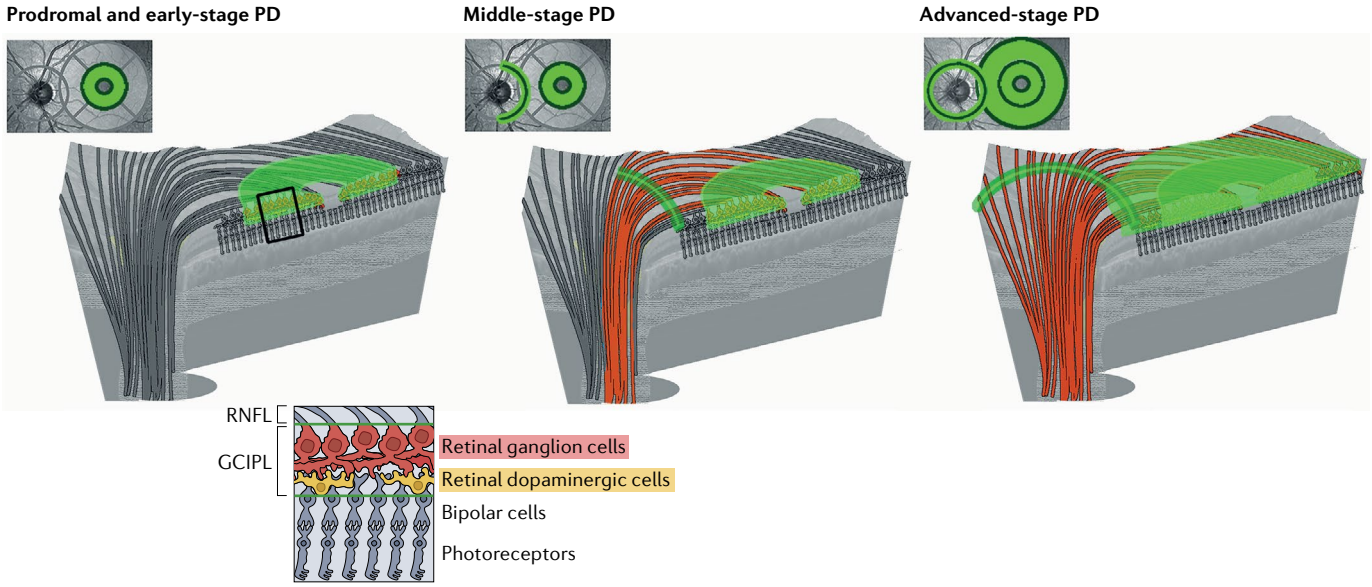

Fig. 5 | **Proposed retinal changes in PD identified by optical coherence tomography.** In the prodromal phase and early-stage Parkinson disease (PD), atrophy (orange shading) of the ganglion cell–inner plexiform layer (GCIPL) complex is detected in the parafoveal region of the macula. The GCIPL complex includes the cell bodies of ganglion cells and dopaminergic cells of the retina, among other retinal structures. In middle-stage PD, in addition to parafoveal GCIPL atrophy, atrophy of the temporal sector of the peripapillary nerve fibre layer (pRNFL), which contains the axons of the ganglion cells of the macula, is identified. In advanced-stage PD, a greater degree of retinal damage is observed, with global atrophy of the entire macular GCIPL and the pRNFL. Of note, along with thinning of the inner retinal layers, fovea avascular zone remodelling is also suggested to occur in PD (not shown).

SNCA mutation — as a reference. This work showed that thinning of the macular area in Lewy body diseases primarily affects the parafoveal GCIPL and correlates with visual cognitive functioning, as assessed by a predefined battery of primary visual function and neuropsychological tests[16]. Thinning of the parafovea is also associated with a more severe clinical phenotype[16], suggesting that parafoveal GCIPL atrophy signifies a clinical subtype of PD with a poor prognosis.

Remodelling of the foveal avascular zone. One study found that the FAZ was reduced in size in people with PD[228], but the precise mechanisms mediating this change are still unknown. The authors suggested that damage to retinal dopaminergic neurons could promote lengthening of foveal capillaries. This retinal change is very similar to that found in the SNc of patients with PD[231], who display 2.5-fold higher vascular endothelial cell counts than controls. More recently, an in vitro study demonstrated that RGCs promote their own survival by releasing vascular endothelial growth factor (VEGF)[232] — a trophic factor that also promotes vasculogenesis. This possible pathogenic feature of PD is supported by experimental studies showing angiogenesis and increased VEGF expression in patients with PD and animal models[233–235]. Alternatively, FAZ reduction could be the consequence of foveal architecture remodelling, with parafoveal thinning and subsequent centrifugal migration of vessels determining the size of the FAZ. Future studies could benefit from OCT angiography to non-invasively ascertain whether vascular changes occur in the macula and optic nerve of patients with PD.

The retrobulbar optic nerve. The retrobulbar optic nerve is formed from the axonal fibre bundles of RGCs and is a key transmission pathway of visual information from the retina to the brain. Several DTI studies have shown microstructural alterations in the optic nerves of patients with PD[20,170,236]. In one study, optic nerve alterations, manifesting as reduced fractional anisotropy or increased diffusivity, correlated with inner retina GCIPL thinning in the macula[20], supporting the hypothesis that retinal pathology is transmitted to various brain structures, including the brainstem, via the optic nerves. Interestingly, both the optic nerve alterations and inner retinal thinning in patients with early-stage PD correlated with gait and freezing scores and sleep and fatigue scores, as measured by the MDS-UPDRS[20], although these data require replication in studies with larger sample sizes. The possibility of crosstalk between the retina and brain during PD progression is also implied by DTI and volumetric studies on primary visual pathways in PD patients with and without visual hallucinations in the absence of dementia[236]. Attempts are underway to understand the trajectory of pathological progression in PD through integrative analysis of retinal and brain changes[237].

Longitudinal studies

Accurate visual perception and processing requires both bottom-up visual afferent information and top-down cognitive control. Interest in vision research in PD is growing, partially in response to compelling evidence that visual impairment is a clinical marker of cognitive deterioration in people with the disease[18,238–240]. To date,

only a few longitudinal OCT studies have been conducted in people with PD. One study found progressive macular thinning in a small ($n = 19$) sample of patients with early-stage PD during an 18-month follow-up period[136].

Murueta-Goyena et al. conducted a 3-year follow-up study[18] in 50 patients with PD (baseline disease duration 6.5 ± 4.0 years) who had participated in an earlier cross-sectional study[16]. The authors found that retinal thinning was most marked in the parafoveal ring in these individuals. Reduced parafoveal GCIPL thickness at baseline was associated with a threefold increased relative risk of cognitive deterioration, defined as a Montreal Cognitive Assessment score reduction of ≥4 points over the 3-year period, but no clear risk elevation for progression of motor impairment[18]. In this study sample, motor progression was defined as an increase of ≥5 points in the UPDRS part III score in the 'on'-medication state, but the authors did not report whether any of the participants had motor fluctuations.

Longitudinal clinical follow-up studies have consistently shown that pRNFL thinning[224] or impaired contrast sensitivity[241] predict early cognitive deterioration in PD. Therefore, retinal atrophy could be an early event that precedes dementia or, alternatively, visual afferent defects might precipitate cognitive deterioration in patients with PD. Standardized visual tests and multifactorial analysis would provide further insight into the underlying mechanisms of visual information processing dysfunction and cognitive worsening in PD. Furthermore, longitudinal studies with longer follow-up periods are needed to clarify the relationship between progression of parafoveal thinning, which might reflect dopaminergic degeneration, and progression of parkinsonism in early-stage PD. Further research is also warranted to explore possible correlations between retinal changes and sleep–wake disturbances or sleep-related disorders in PD.

Future perspectives on retinal imaging

Accumulating evidence suggests that the retina is involved in PD from the early disease stages. The value of non-invasive retinal imaging might be increased if protocols are systematically designed for large cohorts across various disease stages, including the prodromal phase, and the analysis is focused on the parafoveal region rather than the whole macula. Newer retinal imaging techniques such as adaptive optics[242,243], which can visualize cellular-level changes, and OCT angiography[244,245], could also enhance diagnostic utility in PD. In addition, molecular imaging approaches that target retinal amyloid[246] p-αSC or dopaminergic cells, and techniques applying DARC (detection of apoptosing retinal cells) real-time imaging of single neuronal cell apoptosis[247–249] might be developed for early differential diagnosis and monitoring of therapeutic effects in PD and other neurodegenerative diseases. Current and future retinal imaging techniques could enhance our understanding of PD pathogenesis and reveal the complex interactions between retinal and CNS pathology, which lead to various clinical manifestations during disease progression.

Conclusions and future perspectives

The pros and cons of nigral MRI, PET and SPECT imaging and retinal OCT for biomarker development in PD are summarized in TABLE 1. Advanced MRI using diffusion, iron-sensitive and neuromelanin-sensitive sequences can detect microstructural brain alterations in PD, including increased free water in the posterior substantia nigra, increased iron in the SNc, loss of N1 in the substantia nigra, and ventral posterior neuromelanin loss in the SNc. Loss of N1 and neuromelanin volume could be a marker of prodromal and early PD, and multimodal MRI analysis including neuromelanin volume can enhance diagnostic accuracy. Progressive free water

Table 1 | **Pros and cons of brain and retinal imaging techniques in PD**

Feature or application	Free water with diffusion	Iron-sensitive MRI (QSM)	Iron-sensitive MRI (N1 loss)	Neuromelanin-sensitive MRI	Nigrostriatal (DA) PET–SPECT	Extranigral (non-DA) PET–SPECT	Retinal OCT
Supports PD diagnostic criteria[21]	No	No	No	No	Yes: absolute exclusion if scan is normal	Yes: supportive if abnormal ^{123}I-MIBG scintigraphy	No
Accessibility	Moderate[a]	Moderate[a]	Moderate[a]	Moderate[a]	Poor	Extremely poor	Good
Standardized protocols available	No	No	No	No	Yes	Yes (for ^{123}I-MIBG scintigraphy)	No
Cost	Moderate	Moderate	Moderate	Moderate	Expensive	Expensive	Relatively cheap
Potential radiation hazard	No	No	No	No	Yes	Yes	No
Total time for data acquisition	10–40 min	10–40 min	10–40 min	10–40 min	Usually >1 h	Usually >1 h	~10 min
Early diagnosis, prodromal PD	Maybe	Maybe	Yes	Yes	Yes	Yes	Yes
Monitoring disease progression	Yes	Controversial	No data	Yes	Yes	No data	Yes
Prognosis	No data	No data	No data	No data	Yes	No data	Yes

^{123}I-MIBG, ^{123}I-metaiodobenzylguanidine; DA, dopaminergic; N1, nigrosome 1; OCT, optical coherence tomography; PD, Parkinson disease; QSM, quantitative susceptibility mapping; SPECT, single-photon emission CT. [a]Requires compatible MRI scanner with special scan parameters.

increase or neuromelanin loss can also be used to monitor disease progression in patients with early-stage PD. However, multimodal analyses involving MRI and DAT imaging indicate that striatal DAT changes manifest earlier than nigral MRI changes, and DAT imaging is currently favoured over nigral MRI in terms of diagnostic performance. Interestingly, nigral MRI signals and DAT loss are not always congruent, and prognostic studies with nigral MRI signals are currently lacking.

Retinal OCT studies have been used to visualize structural changes in the inner retina in people with PD, including parafoveal thinning in prodromal and early-stage PD, as well as FAZ remodelling. Parafoveal change in PD correlated with nigrostriatal dopaminergic reduction, and associations were also observed between retinal thinning and poor prognostic signs in PD, such as postural instability–gait disorder, cognitive impairment and visual hallucinations. Longitudinal studies have shown progressive retinal thinning; therefore, retinal OCT measures could provide cheap and convenient markers for monitoring disease progression through repeated scanning. However, multicentre large longitudinal studies are required to validate the OCT measures for wider use in PD clinical practice.

Combined non-invasive imaging of early pathological changes in the substantia nigra and retinal parafovea is a promising strategy for future imaging biomarker development in PD. The combination of nigral MRI and retinal OCT might improve diagnostic performance and provide information regarding both disease progression and prognosis — an important unmet need in PD imaging. Furthermore, investigations into the relationship between pathological processes in the retina and pathological processes in the substantia nigra could provide novel insights into the pathogenesis of PD. Longitudinal multimodal imaging studies in prodromal and early-stage PD will be required to explore the potential of this approach.

Published online: 17 February 2022

1. Del Tredici, K. & Braak, H. Review: Sporadic Parkinson's disease: development and distribution of α-synuclein pathology. *Neuropathol. Appl. Neurobiol.* **42**, 33–50 (2016).
2. Horsager, J. et al. Brain-first versus body-first Parkinson's disease: a multimodal imaging case-control study. *Brain* **143**, 3077–3088 (2020).
3. Braak, H. & Del Tredici, K. Neuropathological staging of brain pathology in sporadic Parkinson's disease: separating the wheat from the chaff. *J. Parkinsons Dis.* **7**, S71–S85 (2017).
4. Berg, D. et al. Changing the research criteria for the diagnosis of Parkinson's disease: obstacles and opportunities. *Lancet Neurol.* **12**, 514–524 (2013).
5. London, A., Benhar, I. & Schwartz, M. The retina as a window to the brain–from eye research to CNS disorders. *Nat. Rev. Neurol.* **9**, 44–53 (2013).
6. De Groef, L. & Cordeiro, M. F. Is the eye an extension of the brain in central nervous system disease? *J. Ocul. Pharmacol. Ther.* **34**, 129–133 (2018).
7. Harnois, C. & Di Paolo, T. Decreased dopamine in the retinas of patients with Parkinson's disease. *Invest. Ophthalmol. Vis. Sci.* **31**, 2473–2475 (1990).
8. Witkovsky, P. Dopamine and retinal function. *Doc. Ophthalmol.* **108**, 17–40 (2004).
9. Bodis-Wollner, I. et al. Visual dysfunction in Parkinson's disease. Loss in spatiotemporal contrast sensitivity. *Brain* **110**, 1675–1698 (1987).
10. Hutton, J. T., Morris, J. L. & Elias, J. W. Levodopa improves spatial contrast sensitivity in Parkinson's disease. *Arch. Neurol.* **50**, 721–724 (1993).
11. Lee, J. Y. et al. Retina thickness as a marker of neurodegeneration in prodromal lewy body disease. *Mov. Disord.* **35**, 349–354 (2020).
12. Ortuño-Lizarán, I. et al. Dopaminergic retinal cell loss and visual dysfunction in Parkinson disease. *Ann. Neurol.* **88**, 893–906 (2020).
13. Ortuño-Lizarán, I. et al. Phosphorylated α-synuclein in the retina is a biomarker of Parkinson's disease pathology severity. *Mov. Disord.* **33**, 1315–1324 (2018).
14. Baksi, S. & Singh, N. α-Synuclein impairs ferritinophagy in the retinal pigment epithelium: implications for retinal iron dyshomeostasis in Parkinson's disease. *Sci. Rep.* **7**, 12843 (2017).
15. Mammadova, N. et al. Accelerated accumulation of retinal α-synuclein (pSer129) and tau, neuroinflammation, and autophagic dysregulation in a seeded mouse model of Parkinson's disease. *Neurobiol. Dis.* **121**, 1–16 (2019).
16. Murueta-Goyena, A. et al. Parafoveal thinning of inner retina is associated with visual dysfunction in Lewy body diseases. *Mov. Disord.* **34**, 1315–1324 (2019).
17. Lee, J. Y. et al. Retinal nerve fiber layer thickness and visual hallucinations in Parkinson's disease. *Mov. Disord.* **29**, 61–67 (2014).
18. Murueta-Goyena, A. et al. Retinal thickness predicts the risk of cognitive decline in Parkinson disease. *Ann. Neurol.* **89**, 165–176 (2021).
19. Ahn, J. et al. Retinal thinning associates with nigral dopaminergic loss in de novo Parkinson disease. *Neurology* **91**, e1003–e1012 (2018).
20. Lee, J. Y. et al. Macular ganglion-cell-complex layer thinning and optic nerve integrity in drug-naive Parkinson's disease. *J. Neural Transm.* **126**, 1695–1699 (2019).
21. Postuma, R. B. et al. MDS clinical diagnostic criteria for Parkinson's disease. *Mov. Disord.* **30**, 1591–1601 (2015).
22. Dahlstrom, A. & Fuxe, K. Localization of monoamines in the lower brain stem. *Experientia* **20**, 398–399 (1964).
23. Ma, L. J. et al. Progressive changes in the retinal structure of patients with Parkinson's disease. *J. Parkinsons Dis.* **8**, 85–92 (2018).
24. Damier, P., Hirsch, E. C., Agid, Y. & Graybiel, A. M. The substantia nigra of the human brain. II. Patterns of loss of dopamine-containing neurons in Parkinson's disease. *Brain* **122**, 1437–1448 (1999).
25. Lehericy, S., Bardinet, E., Poupon, C., Vidailhet, M. & Francois, C. 7 Tesla magnetic resonance imaging: a closer look at substantia nigra anatomy in Parkinson's disease. *Mov. Disord.* **29**, 1574–1581 (2014).
26. Jellinger, K. A. Neuropathology of sporadic Parkinson's disease: evaluation and changes of concepts. *Mov. Disord.* **27**, 8–30 (2012).
27. Fearnley, J. M. & Lees, A. J. Ageing and Parkinson's disease: substantia nigra regional selectivity. *Brain* **114**, 2283–2301 (1991).
28. Carballo-Carbajal, I. et al. Brain tyrosinase overexpression implicates age-dependent neuromelanin production in Parkinson's disease pathogenesis. *Nat. Commun.* **10**, 973 (2019).
29. Beach, T. G. et al. Substantia nigra Marinesco bodies are associated with decreased striatal expression of dopaminergic markers. *J. Neuropathol. Exp. Neurol.* **63**, 329–337 (2004).
30. Kuusisto, E., Parkkinen, L. & Alafuzoff, I. Morphogenesis of Lewy bodies: dissimilar incorporation of α-synuclein, ubiquitin, and p62. *J. Neuropathol. Exp. Neurol.* **62**, 1241–1253 (2003).
31. Atkinson-Clement, C., Pinto, S., Eusebio, A. & Coulon, O. Diffusion tensor imaging in Parkinson's disease: review and meta-analysis. *Neuroimage Clin.* **16**, 98–110 (2017).
32. Loane, C. et al. Aberrant nigral diffusion in Parkinson's disease: a longitudinal diffusion tensor imaging study. *Mov. Disord.* **31**, 1020–1026 (2016).
33. Vaillancourt, D. E. et al. High-resolution diffusion tensor imaging in the substantia nigra of de novo Parkinson disease. *Neurology* **72**, 1378–1384 (2009).
34. Pasternak, O., Sochen, N., Gur, Y., Intrator, N. & Assaf, Y. Free water elimination and mapping from diffusion MRI. *Magn. Reson. Med.* **62**, 717–730 (2009).
35. Ofori, E. et al. Increased free water in the substantia nigra of Parkinson's disease: a single-site and multi-site study. *Neurobiol. Aging* **36**, 1097–1104 (2015).
36. Ofori, E. et al. Longitudinal changes in free-water within the substantia nigra of Parkinson's disease. *Brain* **138**, 2322–2331 (2015).
37. Burciu, R. G. et al. Progression marker of Parkinson's disease: a 4-year multi-site imaging study. *Brain* **140**, 2183–2192 (2017).
38. Zhou, L. et al. Increased free water in the substantia nigra in idiopathic REM sleep behaviour disorder. *Brain* **144**, 1488–1497 (2021).
39. Guttuso, T. Jr. et al. Substantia nigra free water increases longitudinally in Parkinson disease. *Am. J. Neuroradiol.* **39**, 479–484 (2018).
40. Arribarat, G. et al. Substantia nigra locations of iron-content, free-water and mean diffusivity abnormalities in moderate stage Parkinson's disease. *Parkinsonism Relat. Disord.* **65**, 146–152 (2019).
41. Planetta, P. J. et al. Free-water imaging in Parkinson's disease and atypical parkinsonism. *Brain* **139**, 495–508 (2016).
42. Prodoehl, J. et al. Diffusion tensor imaging of Parkinson's disease, atypical parkinsonism, and essential tremor. *Mov. Disord.* **28**, 1816–1822 (2013).
43. Andica, C. et al. Neurite orientation dispersion and density imaging of the nigrostriatal pathway in Parkinson's disease: retrograde degeneration observed by tract-profile analysis. *Parkinsonism Relat. Disord.* **51**, 55–60 (2018).
44. Kamagata, K. et al. Neurite orientation dispersion and density imaging in the substantia nigra in idiopathic Parkinson disease. *Eur. Radiol.* **26**, 2567–2577 (2016).
45. Mitchell, T. et al. Neurite orientation dispersion and density imaging (NODDI) and free-water imaging in Parkinsonism. *Hum. Brain Mapp.* **40**, 5094–5107 (2019).
46. Archer, D. B. et al. Development and validation of the automated imaging differentiation in parkinsonism (AID-P): a multicentre machine learning study. *Lancet Digit. Health* **1**, e222–e231 (2019).
47. Dexter, D. T. et al. Increased nigral iron content in postmortem parkinsonian brain. *Lancet* **2**, 1219–1220 (1987).
48. Hallgren, B. & Sourander, P. The effect of age on the non-haemin iron in the human brain. *J. Neurochem.* **3**, 41–51 (1958).
49. Haacke, E. M. et al. Imaging iron stores in the brain using magnetic resonance imaging. *Magn. Reson. Imaging* **23**, 1–25 (2005).
50. Pietracupa, S., Martin-Bastida, A. & Piccini, P. Iron metabolism and its detection through MRI in parkinsonian disorders: a systematic review. *Neurol. Sci.* **38**, 2095–2101 (2017).
51. Wang, J. Y. et al. Meta-analysis of brain iron levels of Parkinson's disease patients determined by postmortem and MRI measurements. *Sci. Rep.* **6**, 36669 (2016).

52. Sun, J. et al. Quantitative evaluation of iron content in idiopathic rapid eye movement sleep behavior disorder. *Mov. Disord.* **35**, 478–485 (2020).
53. Langley, J. et al. Reproducible detection of nigral iron deposition in 2 Parkinson's disease cohorts. *Mov. Disord.* **34**, 416–419 (2019).
54. Langley, J., Huddleston, D. E., Sedlacik, J., Boelmans, K. & Hu, X. P. Parkinson's disease-related increase of T2*-weighted hypointensity in substantia nigra pars compacta. *Mov. Disord.* **32**, 441–449 (2017).
55. Bergsland, N. et al. Ventral posterior substantia nigra iron increases over 3 years in Parkinson's disease. *Mov. Disord.* **34**, 1006–1013 (2019).
56. Barbosa, J. H. et al. Quantifying brain iron deposition in patients with Parkinson's disease using quantitative susceptibility mapping, R2 and R2. *Magn. Reson. Imaging* **33**, 559–565 (2015).
57. Acosta-Cabronero, J. et al. The whole-brain pattern of magnetic susceptibility perturbations in Parkinson's disease. *Brain* **140**, 118–131 (2017).
58. Thomas, G. E. C. et al. Brain iron deposition is linked with cognitive severity in Parkinson's disease. *J. Neurol. Neurosurg. Psychiatry* **91**, 418–425 (2020).
59. Ulla, M. et al. Is R2* a new MRI biomarker for the progression of Parkinson's disease? A longitudinal follow-up. *PLoS ONE* **8**, e57904 (2013).
60. Wieler, M., Gee, M. & Martin, W. R. Longitudinal midbrain changes in early Parkinson's disease: iron content estimated from R2*/MRI. *Parkinsonism Relat. Disord.* **21**, 179–183 (2015).
61. Schwarz, S. T. et al. The 'swallow tail' appearance of the healthy nigrosome–a new accurate test of Parkinson's disease: a case–control and retrospective cross-sectional MRI study at 3T. *PLoS ONE* **9**, e93814 (2014).
62. Schwarz, S. T. et al. Parkinson's disease related signal change in the nigrosomes 1–5 and the substantia nigra using T2* weighted 7T MRI. *Neuroimage Clin.* **19**, 683–689 (2018).
63. Kim, J. M. et al. Loss of substantia nigra hyperintensity on 7 Tesla MRI of Parkinson's disease, multiple system atrophy, and progressive supranuclear palsy. *Parkinsonism Relat. Disord.* **26**, 47–54 (2016).
64. Bae, Y. J. et al. Loss of substantia nigra hyperintensity at 3.0-T MR imaging in idiopathic REM sleep behavior disorder: comparison with (123)I-FP-CIT SPECT. *Radiology* **287**, 285–293 (2018).
65. De Marzi, R. et al. Loss of dorsolateral nigral hyperintensity on 3.0 tesla susceptibility-weighted imaging in idiopathic rapid eye movement sleep behavior disorder. *Ann. Neurol.* **79**, 1026–1030 (2016).
66. Frosini, D. et al. Seven tesla MRI of the substantia nigra in patients with rapid eye movement sleep behavior disorder. *Parkinsonism Relat. Disord.* **43**, 105–109 (2017).
67. Reiter, E. et al. Dorsolateral nigral hyperintensity on 3.0T susceptibility-weighted imaging in neurodegenerative Parkinsonism. *Mov. Disord.* **30**, 1068–1076 (2015).
68. Bae, Y. J. et al. Loss of nigral hyperintensity on 3 Tesla MRI of parkinsonism: comparison with (123)I-FP-CIT SPECT. *Mov. Disord.* **31**, 684–692 (2016).
69. An, H. et al. Quantifying iron deposition within the substantia nigra of Parkinson's disease by quantitative susceptibility mapping. *J. Neurol. Sci.* **386**, 46–52 (2018).
70. Bae, Y. J. et al. Comparison of susceptibility-weighted imaging and susceptibility map-weighted imaging for the diagnosis of Parkinsonism with nigral hyperintensity. *Eur. J. Radiol.* **134**, 109398 (2021).
71. Cheng, Z. et al. Imaging the nigrosome 1 in the substantia nigra using susceptibility weighted imaging and quantitative susceptibility mapping: an application to Parkinson's disease. *Neuroimage Clin.* **25**, 102103 (2020).
72. Nam, Y., Gho, S. M., Kim, D. H., Kim, E. Y. & Lee, J. Imaging of nigrosome 1 in substantia nigra at 3T using multiecho susceptibility map-weighted imaging (SMWI). *J. Magn. Reson. Imaging* **46**, 528–536 (2017).
73. Kim, E. Y. et al. Diagnosis of early-stage idiopathic Parkinson's disease using high-resolution quantitative susceptibility mapping combined with histogram analysis in the substantia nigra at 3 T. *J. Clin. Neurol.* **14**, 90–97 (2018).
74. Barber, T. R. et al. Nigrosome 1 imaging in REM sleep behavior disorder and its association with dopaminergic decline. *Ann. Clin. Transl. Neurol.* **7**, 26–35 (2020).
75. Reimao, S., Guerreiro, C., Seppi, K., Ferreira, J. J. & Poewe, W. A standardized MR imaging protocol for parkinsonism. *Mov. Disord.* **35**, 1745–1750 (2020).
76. Fedorow, H. et al. Neuromelanin in human dopamine neurons: comparison with peripheral melanins and relevance to Parkinson's disease. *Prog. Neurobiol.* **75**, 109–124 (2005).
77. Sulzer, D. et al. Neuromelanin biosynthesis is driven by excess cytosolic catecholamines not accumulated by synaptic vesicles. *Proc. Natl Acad. Sci. USA* **97**, 11869–11874 (2000).
78. Zecca, L. et al. Neuromelanin can protect against iron-mediated oxidative damage in system modeling iron overload of brain aging and Parkinson's disease. *J. Neurochem.* **106**, 1866–1875 (2008).
79. Zhang, W. et al. Neuromelanin activates microglia and induces degeneration of dopaminergic neurons: implications for progression of Parkinson's disease. *Neurotox. Res.* **19**, 63–72 (2011).
80. Sulzer, D. et al. Neuromelanin detection by magnetic resonance imaging (MRI) and its promise as a biomarker for Parkinson's disease. *npj Parkinson's Dis.* **4**, 11 (2018).
81. Chen, X. et al. Simultaneous imaging of locus coeruleus and substantia nigra with a quantitative neuromelanin MRI approach. *Magn. Reson. Imaging* **32**, 1301–1306 (2014).
82. Schwarz, S. T. et al. T1-weighted MRI shows stage-dependent substantia nigra signal loss in Parkinson's disease. *Mov. Disord.* **26**, 1633–1638 (2011).
83. Ohtsuka, C. et al. Changes in substantia nigra and locus coeruleus in patients with early-stage Parkinson's disease using neuromelanin-sensitive MR imaging. *Neurosci. Lett.* **541**, 93–98 (2013).
84. Fabbri, M. et al. Substantia nigra neuromelanin as an imaging biomarker of disease progression in Parkinson's disease. *J. Parkinsons Dis.* **7**, 491–501 (2017).
85. Reimao, S. et al. Substantia nigra neuromelanin magnetic resonance imaging in de novo Parkinson's disease patients. *Eur. J. Neurol.* **22**, 540–546 (2015).
86. Wang, J. et al. Neuromelanin-sensitive magnetic resonance imaging features of the substantia nigra and locus coeruleus in de novo Parkinson's disease and its phenotypes. *Eur. J. Neurol.* **25**, 949-e73 (2018).
87. Matsuura, K. et al. Neuromelanin magnetic resonance imaging in Parkinson's disease and multiple system atrophy. *Eur. Neurol.* **70**, 70–77 (2013).
88. Ohtsuka, C. et al. Differentiation of early-stage parkinsonisms using neuromelanin-sensitive magnetic resonance imaging. *Parkinsonism Relat. Disord.* **20**, 755–760 (2014).
89. Schwarz, S. T., Xing, Y., Tomar, P., Bajaj, N. & Auer, D. P. In vivo assessment of brainstem depigmentation in Parkinson disease: potential as a severity marker for multicenter studies. *Radiology* **283**, 789–798 (2017).
90. Biondetti, E. et al. Spatiotemporal changes in substantia nigra neuromelanin content in Parkinson's disease. *Brain* **143**, 2757–2770 (2020).
91. Gaurav, R. et al. Longitudinal changes in neuromelanin MRI signal in Parkinson's disease: a progression marker. *Mov. Disord.* **36**, 1592–1602 (2021).
92. Matsuura, K. et al. A longitudinal study of neuromelanin-sensitive magnetic resonance imaging in Parkinson's disease. *Neurosci. Lett.* **633**, 112–117 (2016).
93. Garcia-Lorenzo, D. et al. The coeruleus/subcoeruleus complex in rapid eye movement sleep behaviour disorders in Parkinson's disease. *Brain* **136**, 2120–2129 (2013).
94. Ehrminger, M. et al. The coeruleus/subcoeruleus complex in idiopathic rapid eye movement sleep behaviour disorder. *Brain* **139**, 1180–1188 (2016).
95. Knudsen, K. et al. In-vivo staging of pathology in REM sleep behaviour disorder: a multimodality imaging case-control study. *Lancet Neurol.* **17**, 618–628 (2018).
96. Pyatigorskaya, N. et al. Magnetic resonance imaging biomarkers to assess substantia nigra damage in idiopathic rapid eye movement sleep behavior disorder. *Sleep* **40**, zsx149 (2017).
97. Langley, J. et al. Diffusion tensor imaging of the substantia nigra in Parkinson's disease revisited. *Hum. Brain Mapp.* **37**, 2547–2556 (2016).
98. Safai, A. et al. Microstructural abnormalities of substantia nigra in Parkinson's disease: a neuromelanin sensitive MRI atlas based study. *Hum. Brain Mapp.* **41**, 1323–1333 (2020).
99. He, N. et al. Imaging iron and neuromelanin simultaneously using a single 3D gradient echo magnetization transfer sequence: combining neuromelanin, iron and the nigrosome-1 sign as complementary imaging biomarkers in early stage Parkinson's disease. *Neuroimage* **230**, 117810 (2021).
100. Perez Akly, M. S. et al. Accuracy of nigrosome-1 detection to discriminate patients with Parkinson's disease and essential tremor. *Neuroradiol. J.* **32**, 395–400 (2019).
101. Wang, J. et al. Neuromelanin-sensitive MRI of the substantia nigra: an imaging biomarker to differentiate essential tremor from tremor-dominant Parkinson's disease. *Parkinsonism Relat. Disord.* **58**, 3–8 (2019).
102. Jin, L. et al. Combined visualization of nigrosome-1 and neuromelanin in the substantia nigra using 3T MRI for the differential diagnosis of essential tremor and de novo Parkinson's disease. *Front. Neurol.* **10**, 100 (2019).
103. Nandhagopal, R. et al. Longitudinal evolution of compensatory changes in striatal dopamine processing in Parkinson's disease. *Brain* **134**, 3290–3298 (2011).
104. de la Fuente-Fernandez, R. et al. Age-specific progression of nigrostriatal dysfunction in Parkinson's disease. *Ann. Neurol.* **69**, 803–810 (2011).
105. Shin, J. H. et al. Longitudinal change in dopamine transporter availability in idiopathic REM sleep behavior disorder. *Neurology* **95**, e3081–e3092 (2020).
106. Iranzo, A. et al. Serial dopamine transporter imaging of nigrostriatal function in patients with idiopathic rapid-eye-movement sleep behaviour disorder: a prospective study. *Lancet Neurol.* **10**, 797–805 (2011).
107. Seibyl, J. & Cheng, D. Four year longitudinal assessment of DAT imaging biomarkers in a progressing Parkinson disease cohort: analysis strategies and implications for treatment trial design [abstract]. *J. Nucl. Med.* **59** (Suppl. 1), 628 (2018).
108. Iranzo, A. et al. Dopamine transporter imaging deficit predicts early transition to synucleinopathy in idiopathic rapid eye movement sleep behavior disorder. *Ann. Neurol.* **82**, 419–428 (2017).
109. Jennings, D. et al. Conversion to Parkinson disease in the PARS hyposmic and dopamine transporter-deficit prodromal cohort. *JAMA Neurol.* **74**, 933–940 (2017).
110. Lenfeldt, N., Eriksson, J., Astrom, B., Forsgren, L. & Mo, S. J. Fractional anisotropy and mean diffusion as measures of dopaminergic function in Parkinson's disease: challenging results. *J. Parkinsons Dis.* **7**, 129–142 (2017).
111. Isaias, I. U. et al. Neuromelanin imaging and dopaminergic loss in Parkinson's disease. *Front. Aging Neurosci.* **8**, 196 (2016).
112. Kuya, K. et al. Evaluation of Parkinson's disease by neuromelanin-sensitive magnetic resonance imaging and (123)I-FP-CIT SPECT. *Acta Radiol.* **59**, 593–598 (2018).
113. Martin-Bastida, A. et al. Relationship between neuromelanin and dopamine terminals within the Parkinson's nigrostriatal system. *Brain* **142**, 2023–2036 (2019).
114. Saari, L. et al. Dopamine transporter imaging does not predict the number of nigral neurons in Parkinson disease. *Neurology* **88**, 1461–1467 (2017).
115. Karimi, M. et al. Validation of nigrostriatal positron emission tomography measures: critical limits. *Ann. Neurol.* **73**, 390–396 (2013).
116. Kordower, J. H. et al. Disease duration and the integrity of the nigrostriatal system in Parkinson's disease. *Brain* **136**, 2419–2431 (2013).
117. Biondetti, E. et al. The spatiotemporal changes in dopamine, neuromelanin and iron characterizing Parkinson's disease. *Brain* **144**, 3114–3125 (2021).
118. Tatton, W. G., Kwan, M. M., Verrier, M. C., Seniuk, N. A. & Theriault, E. MPTP produces reversible disappearance of tyrosine hydroxylase-containing retinal amacrine cells. *Brain Res.* **527**, 21–31 (1990).
119. Meng, T., Zheng, Z. H., Liu, T. T. & Lin, L. Contralateral retinal dopamine decrease and melatonin increase in progression of hemiparkinsonium rat. *Neurochem. Res.* **37**, 1050–1056 (2012).
120. Esteve-Rudd, J. et al. Rotenone induces degeneration of photoreceptors and impairs the dopaminergic system in the rat retina. *Neurobiol. Dis.* **44**, 102–115 (2011).
121. Kolb, H., Cuenca, N., Wang, H. H. & Dekorver, L. The synaptic organization of the dopaminergic

amacrine cell in the cat retina. *J. Neurocytol.* **19**, 343–366 (1990).
122. Popova, E. The role of dopamine in retinal function. *Webvision* https://webvision.med.utah.edu/book/part-iv-neurotransmitters-in-the-retina-2/the-role-of-dopamine-in-retinal-function-by-elka-popova/ (2021).
123. Bodis-Wollner, I. & Yahr, M. D. Measurements of visual evoked potentials in Parkinson's disease. *Brain* **101**, 661–671 (1978).
124. Jeon, B. S., Lee, K. W., Lee, S. B. & Myung, H. J. Flash ERG findings in Parkinson's disease. *J. Korean Neurol. Assoc.* **5**, 7 (1987).
125. Garcia-Martin, E. et al. Electrophysiology and optical coherence tomography to evaluate Parkinson disease severity. *Invest. Ophthalmol. Vis. Sci.* **55**, 696–705 (2014).
126. Langheinrich, T. et al. Visual contrast response functions in Parkinson's disease: evidence from electroretinograms, visually evoked potentials and psychophysics. *Clin. Neurophysiol.* **111**, 66–74 (2000).
127. Moschos, M. M. et al. Morphologic changes and functional retinal impairment in patients with Parkinson disease without visual loss. *Eur. J. Ophthalmol.* **21**, 24–29 (2011).
128. Peppe, A. et al. Low contrast stimuli enhance PERG sensitivity to the visual dysfunction in Parkinson's disease. *Electroencephalogr. Clin. Neurophysiol.* **82**, 453–457 (1992).
129. Tagliati, M., Bodis-Wollner, I. & Yahr, M. D. The pattern electroretinogram in Parkinson's disease reveals lack of retinal spatial tuning. *Electroencephalogr. Clin. Neurophysiol.* **100**, 1–11 (1996).
130. Stanzione, P. et al. Pattern visual evoked potentials and electroretinogram abnormalities in Parkinson's disease: effects of L-dopa therapy. *Clin. Vis. Sci.* **4**, 115–127 (1989).
131. Bodis-Wollner, I. & Tzelepi, A. The push-pull action of dopamine on spatial tuning of the monkey retina: the effects of dopaminergic deficiency and selective D1 and D2 receptor ligands on the pattern electroretinogram. *Vis. Res.* **38**, 1479–1487 (1998).
132. Bulens, C., Meerwaldt, J. D., van der Wildt, G. J. & Keemink, C. J. Visual contrast sensitivity in drug-induced parkinsonism. *J. Neurol. Neurosurg. Psychiatry* **52**, 341–345 (1989).
133. Bodis-Wollner, I. Foveal vision is impaired in Parkinson's disease. *Parkinsonism Relat. Disord.* **19**, 1–14 (2013).
134. Diederich, N. J., Raman, R., Leurgans, S. & Goetz, C. G. Progressive worsening of spatial and chromatic processing deficits in Parkinson disease. *Arch. Neurol.* **59**, 1249–1252 (2002).
135. Silva, M. F. et al. Independent patterns of damage within magno-, parvo- and koniocellular pathways in Parkinson's disease. *Brain* **128**, 2260–2271 (2005).
136. Hasanov, S. et al. Functional and morphological assessment of ocular structures and follow-up of patients with early-stage Parkinson's disease. *Int. Ophthalmol.* **39**, 1255–1262 (2019).
137. Matar, E., Phillips, J. R., Martens, K. A. E., Halliday, G. M. & Lewis, S. J. G. Impaired color discrimination–a specific marker of hallucinations in Lewy body disorders. *J. Geriatr. Psychiatry Neurol.* **32**, 257–264 (2019).
138. Bertrand, J. A. et al. Color discrimination deficits in Parkinson's disease are related to cognitive impairment and white-matter alterations. *Mov. Disord.* **27**, 1781–1788 (2012).
139. Kertelge, L. et al. Impaired sense of smell and color discrimination in monogenic and idiopathic Parkinson's disease. *Mov. Disord.* **25**, 2665–2669 (2010).
140. Oh, Y. S. et al. Color vision in Parkinson's disease and essential tremor. *Eur. J. Neurol.* **18**, 577–583 (2011).
141. Polo, V. et al. Visual dysfunction and its correlation with retinal changes in patients with Parkinson's disease: an observational cross-sectional study. *BMJ Open* **6**, e009658 (2016).
142. Sartucci, F. & Porciatti, V. Visual-evoked potentials to onset of chromatic red-green and blue-yellow gratings in Parkinson's disease never treated with L-dopa. *J. Clin. Neurophysiol.* **23**, 431–435 (2006).
143. Stenc Bradvica, I., Bradvica, M., Matic, S. & Reisz-Majic, P. Visual dysfunction in patients with Parkinson's disease and essential tremor. *Neurol. Sci.* **36**, 257–262 (2015).
144. Buttner, T., Kuhn, W. & Przuntek, H. Alterations in chromatic contour perception in de novo parkinsonian patients. *Eur. Neurol.* **35**, 226–229 (1995).
145. Fereshtehnejad, S. M. et al. New clinical subtypes of Parkinson disease and their longitudinal progression: a prospective cohort comparison with other phenotypes. *JAMA Neurol.* **72**, 863–873 (2015).
146. Haug, B. A., Kolle, R. U., Trenkwalder, C., Oertel, W. H. & Paulus, W. Predominant affection of the blue cone pathway in Parkinson's disease. *Brain* **118**, 771–778 (1995).
147. Muller, T. et al. Colour vision abnormalities do not correlate with dopaminergic nigrostriatal degeneration in Parkinson's disease. *J. Neurol.* **245**, 659–664 (1998).
148. Muller, T., Kuhn, W., Buttner, T. & Przuntek, H. Colour vision abnormalities and movement time in Parkinson's disease. *Eur. J. Neurol.* **6**, 711–715 (1999).
149. Pieri, V., Diederich, N. J., Raman, R. & Goetz, C. G. Decreased color discrimination and contrast sensitivity in Parkinson's disease. *J. Neurol. Sci.* **172**, 7–11 (2000).
150. Postuma, R. B., Gagnon, J. F., Vendette, M., Charland, K. & Montplaisir, J. Manifestations of Parkinson disease differ in association with REM sleep behavior disorder. *Mov. Disord.* **23**, 1665–1672 (2008).
151. Price, M. J., Feldman, R. G., Adelberg, D. & Kayne, H. Abnormalities in color vision and contrast sensitivity in Parkinson's disease. *Neurology* **42**, 887–890 (1992).
152. Regan, B. C., Freudenthaler, N., Kolle, R., Mollon, J. D. & Paulus, W. Colour discrimination thresholds in Parkinson's disease: results obtained with a rapid computer-controlled colour vision test. *Vis. Res.* **38**, 3427–3431 (1998).
153. Satue, M. et al. Evaluation of progressive visual dysfunction and retinal degeneration in patients with Parkinson's disease. *Invest. Ophthalmol. Vis. Sci.* **58**, 1151–1157 (2017).
154. Barbato, L., Rinalduzzi, S., Laurenti, M., Ruggieri, S. & Accornero, N. Color VEPs in Parkinson's disease. *Electroencephalogr. Clin. Neurophysiol.* **92**, 169–172 (1994).
155. Birch, J., Kolle, R. U., Kunkel, M., Paulus, W. & Upadhyay, P. Acquired colour deficiency in patients with Parkinson's disease. *Vis. Res.* **38**, 3421–3426 (1998).
156. Jones, R. D., Donaldson, I. M. & Timmings, P. L. Impairment of high-contrast visual acuity in Parkinson's disease. *Mov. Disord.* **7**, 232–238 (1992).
157. Lin, T. P. et al. Abnormal visual contrast acuity in Parkinson's disease. *J. Parkinsons Dis.* **5**, 125–130 (2015).
158. Gupta, H. V. et al. Contrast acuity with different colors in Parkinson's disease. *Mov. Disord. Clin. Pract.* **6**, 672–677 (2019).
159. Regan, D. & Neima, D. Low-contrast letter charts in early diabetic retinopathy, ocular hypertension, glaucoma, and Parkinson's disease. *Br. J. Ophthalmol.* **68**, 885–889 (1984).
160. Rascol, O. et al. Abnormal ocular movements in Parkinson's disease. Evidence for involvement of dopaminergic systems. *Brain* **112**, 1193–1214 (1989).
161. Terao, Y. et al. Initiation and inhibitory control of saccades with the progression of Parkinson's disease–changes in three major drives converging on the superior colliculus. *Neuropsychologia* **49**, 1794–1806 (2011).
162. Marino, S., Lanzafame, P., Sessa, E., Bramanti, A. & Bramanti, P. The effect of L-Dopa administration on pursuit ocular movements in suspected Parkinson's disease. *Neurol. Sci.* **31**, 381–385 (2010).
163. Stock, L., Kruger-Zechlin, C., Deeb, Z., Timmermann, L. & Waldthaler, J. Natural reading in Parkinson's disease with and without mild cognitive impairment. *Front. Aging Neurosci.* **12**, 120 (2020).
164. Moro, E. et al. Visual dysfunction of the superior colliculus in de novo parkinsonian patients. *Ann. Neurol.* **87**, 533–546 (2020).
165. Archibald, N. K., Clarke, M. P., Mosimann, U. P. & Burn, D. J. The retina in Parkinson's disease. *Brain* **132**, 1128–1145 (2009).
166. Davidsdottir, S., Cronin-Golomb, A. & Lee, A. Visual and spatial symptoms in Parkinson's disease. *Vis. Res.* **45**, 1285–1296 (2005).
167. Pagonabarraga, J. et al. Minor hallucinations occur in drug-naive Parkinson's disease patients, even from the premotor phase. *Mov. Disord.* **31**, 45–52 (2016).
168. Bradley, V. A., Welch, J. L. & Dick, D. J. Visuospatial working memory in Parkinson's disease. *J. Neurol. Neurosurg. Psychiatry* **52**, 1228–1235 (1989).
169. Fernandez-Baizan, C. et al. Patients with Parkinson's disease show alteration in their visuospatial abilities and in their egocentric and allocentric spatial orientation measured by card placing tests. *J. Parkinsons Dis.* **10**, 1807–1816 (2020).
170. Lee, J. J. et al. Optic nerve integrity as a visuospatial cognitive predictor in Parkinson's disease. *Parkinsonism Relat. Disord.* **31**, 41–45 (2016).
171. Bodis-Wollner, I., Kozlowski, P. B., Glazman, S. & Miri, S. α-synuclein in the inner retina in parkinson disease. *Ann. Neurol.* **75**, 964–966 (2014).
172. Beach, T. G. et al. Phosphorylated α-synuclein-immunoreactive retinal neuronal elements in Parkinson's disease subjects. *Neurosci. Lett.* **571**, 34–38 (2014).
173. Cuenca, N. et al. Morphological impairments in retinal neurons of the scotopic visual pathway in a monkey model of Parkinson's disease. *J. Comp. Neurol.* **493**, 261–273 (2005).
174. Deans, M. R., Volgyi, B., Goodenough, D. A., Bloomfield, S. A. & Paul, D. L. Connexin36 is essential for transmission of rod-mediated visual signals in the mammalian retina. *Neuron* **36**, 703–712 (2002).
175. Benarroch, E. E. The melanopsin system: phototransduction, projections, functions, and clinical implications. *Neurology* **76**, 1422–1427 (2011).
176. Fifel, K. & Videnovic, A. Light therapy in Parkinson's disease: towards mechanism-based protocols. *Trends Neurosci.* **41**, 252–254 (2018).
177. Esquiva, G., Lax, P., Perez-Santonja, J. J., Garcia-Fernandez, J. M. & Cuenca, N. Loss of melanopsin-expressing ganglion cell subtypes and dendritic degeneration in the aging human retina. *Front. Aging Neurosci.* **9**, 79 (2017).
178. Ortuño-Lizarán, I. et al. Degeneration of human photosensitive retinal ganglion cells may explain sleep and circadian rhythms disorders in Parkinson's disease. *Acta Neuropathol. Commun.* **6**, 90 (2018).
179. Nguyen-Legros, J. & Hicks, D. Renewal of photoreceptor outer segments and their phagocytosis by the retinal pigment epithelium. *Int. Rev. Cytol.* **196**, 245–313 (2000).
180. Gabriele, M. L. et al. Optical coherence tomography: history, current status, and laboratory work. *Invest. Ophthalmol. Vis. Sci.* **52**, 2425–2436 (2011).
181. Fujimoto, J. & Swanson, E. The development, commercialization, and impact of optical coherence tomography. *Invest. Ophthalmol. Vis. Sci.* **57**, OCT1–OCT13 (2016).
182. Cruz-Herranz, A. et al. The APOSTEL recommendations for reporting quantitative optical coherence tomography studies. *Neurology* **86**, 2303–2309 (2016).
183. Aytulun, A. et al. APOSTEL 2.0 recommendations for reporting quantitative optical coherence tomography studies. *Neurology* **97**, 68–79 (2021).
184. Altintas, O., Iseri, P., Ozkan, B. & Caglar, Y. Correlation between retinal morphological and functional findings and clinical severity in Parkinson's disease. *Doc. Ophthalmol.* **116**, 137–146 (2008).
185. Aydin, T. S. et al. Optical coherence tomography findings in Parkinson's disease. *Kaohsiung J. Med. Sci.* **34**, 166–171 (2018).
186. Eraslan, M. et al. Comparison of optical coherence tomography findings in patients with primary open-angle glaucoma and Parkinson disease. *J. Glaucoma* **25**, e639–e646 (2016).
187. Jimenez, B., Ascaso, F. J., Cristobal, J. A. & Lopez del Val, J. Development of a prediction formula of Parkinson disease severity by optical coherence tomography. *Mov. Disord.* **29**, 68–74 (2014).
188. Kaur, M. et al. Correlation between structural and functional retinal changes in Parkinson disease. *J. Neuroophthalmol.* **35**, 254–258 (2015).
189. Moschos, M. M. & Chatziralli, I. P. Evaluation of choroidal and retinal thickness changes in Parkinson's disease using spectral domain optical coherence tomography. *Semin. Ophthalmol.* **33**, 494–497 (2018).
190. Pilat, A. et al. In vivo morphology of the optic nerve and retina in patients with Parkinson's disease. *Invest. Ophthalmol. Vis. Sci.* **57**, 4420–4427 (2016).
191. Satue, M. et al. Use of Fourier-domain OCT to detect retinal nerve fiber layer degeneration in Parkinson's disease patients. *Eye* **27**, 507–514 (2013).
192. Satue, M. et al. Retinal thinning and correlation with functional disability in patients with Parkinson's disease. *Br. J. Ophthalmol.* **98**, 350–355 (2014).
193. Sengupta, P. et al. Optical coherence tomography findings in patients of Parkinson's disease: an Indian perspective. *Ann. Indian Acad. Neurol.* **21**, 150–155 (2018).
194. Kirbas, S., Turkyilmaz, K., Tufekci, A. & Durmus, M. Retinal nerve fiber layer thickness in Parkinson disease. *J. Neuroophthalmol.* **33**, 62–65 (2013).
195. La Morgia, C. et al. Loss of temporal retinal nerve fibers in Parkinson disease: a mitochondrial pattern? *Eur. J. Neurol.* **20**, 198–201 (2013).

196. Moreno-Ramos, T., Benito-Leon, J., Villarejo, A. & Bermejo-Pareja, F. Retinal nerve fiber layer thinning in dementia associated with Parkinson's disease, dementia with Lewy bodies, and Alzheimer's disease. *J. Alzheimers Dis.* **34**, 659–664 (2013).
197. Ucak, T. et al. Analysis of the retinal nerve fiber and ganglion cell–inner plexiform layer by optical coherence tomography in Parkinson's patients. *Parkinsonism Relat. Disord.* **31**, 59–64 (2016).
198. Rohani, M. et al. Retinal nerve changes in patients with tremor dominant and akinetic rigid Parkinson's disease. *Neurol. Sci.* **34**, 689–693 (2013).
199. Sung, M. S. et al. Inner retinal thinning as a biomarker for cognitive impairment in de novo Parkinson's disease. *Sci. Rep.* **9**, 11832 (2019).
200. Garcia-Martin, E. et al. Ability and reproducibility of Fourier-domain optical coherence tomography to detect retinal nerve fiber layer atrophy in Parkinson's disease. *Ophthalmology* **119**, 2161–2167 (2012).
201. Roth, N. M. et al. Photoreceptor layer thinning in idiopathic Parkinson's disease. *Mov. Disord.* **29**, 1163–1170 (2014).
202. Aaker, G. D. et al. Detection of retinal changes in Parkinson's disease with spectral-domain optical coherence tomography. *Clin. Ophthalmol.* **4**, 1427–1432 (2010).
203. Albrecht, P. et al. Optical coherence tomography in parkinsonian syndromes. *PLoS ONE* **7**, e34891 (2012).
204. Archibald, N. K., Clarke, M. P., Mosimann, U. P. & Burn, D. J. Retinal thickness in Parkinson's disease. *Parkinsonism Relat. Disord.* **17**, 431–436 (2011).
205. Bittersohl, D. et al. Detection of retinal changes in idiopathic Parkinson's disease using high-resolution optical coherence tomography and Heidelberg retina tomography. *Acta Ophthalmol.* **93**, e578–e584 (2015).
206. Chorostecki, J. et al. Characterization of retinal architecture in Parkinson's disease. *J. Neurol. Sci.* **355**, 44–48 (2015).
207. Mailankody, P. et al. Optical coherence tomography as a tool to evaluate retinal changes in Parkinson's disease. *Parkinsonism Relat. Disord.* **21**, 1164–1169 (2015).
208. Nowacka, B., Lubinski, W., Honczarenko, K., Potemkowski, A. & Safranow, K. Bioelectrical function and structural assessment of the retina in patients with early stages of Parkinson's disease (PD). *Doc. Ophthalmol.* **131**, 95–104 (2015).
209. Quagliato, L. B., Domingues, C., Quagliato, E. M., Abreu, E. B. & Kara-Junior, N. Applications of visual evoked potentials and Fourier-domain optical coherence tomography in Parkinson's disease: a controlled study. *Arq. Bras. Oftalmol.* **77**, 238–242 (2014).
210. Tugcu, B. et al. Evaluation of retinal alterations in Parkinson disease and tremor diseases. *Acta Neurol. Belg.* **120**, 107–113 (2020).
211. Yang, Z. J. et al. Retinal nerve fiber layer thinning: a window into rapid eye movement sleep behavior disorders in Parkinson's disease. *Sleep. Breath.* **20**, 1285–1292 (2016).
212. Bayhan, H. A., Aslan Bayhan, S., Tanik, N. & Gurdal, C. The association of spectral-domain optical coherence tomography determined ganglion cell complex parameters and disease severity in Parkinson's disease. *Curr. Eye Res.* **39**, 1117–1122 (2014).
213. Garcia-Martin, E. et al. Distribution of retinal layer atrophy in patients with Parkinson disease and association with disease severity and duration. *Am. J. Ophthalmol.* **157**, 470–478.e2 (2014).
214. Hajee, M. E. et al. Inner retinal layer thinning in Parkinson disease. *Arch. Ophthalmol.* **127**, 737–741 (2009).
215. Unlu, M., Gulmez Sevim, D., Gultekin, M. & Karaca, C. Correlations among multifocal electroretinography and optical coherence tomography findings in patients with Parkinson's disease. *Neurol. Sci.* **39**, 533–541 (2018).
216. Zivkovic, M. et al. Retinal ganglion cell/inner plexiform layer thickness in patients with Parkinson's disease. *Folia Neuropathol.* **55**, 168–173 (2017).
217. Chrysou, A., Jansonius, N. M. & van Laar, T. Retinal layers in Parkinson's disease: a meta-analysis of spectral-domain optical coherence tomography studies. *Parkinsonism Relat. Disord.* **64**, 40–49 (2019).
218. Visser, F. et al. Visual hallucinations in Parkinson's disease are associated with thinning of the inner retina. *Sci. Rep.* **10**, 21110 (2020).
219. Sari, E. S., Koc, R., Yazici, A., Sahin, G. & Ermis, S. S. Ganglion cell-inner plexiform layer thickness in patients with Parkinson disease and association with disease severity and duration. *J. Neuroophthalmol.* **35**, 117–121 (2015).
220. Cubo, E. et al. Lack of association of morphologic and functional retinal changes with motor and non-motor symptoms severity in Parkinson's disease. *J. Neural Transm.* **121**, 139–145 (2014).
221. Matlach, J. et al. Retinal changes in Parkinson's disease and glaucoma. *Parkinsonism Relat. Disord.* **56**, 41–46 (2018).
222. Schneider, M. et al. Retinal single-layer analysis in Parkinsonian syndromes: an optical coherence tomography study. *J. Neural Transm.* **121**, 41–47 (2014).
223. Miri, S., Glazman, S., Mylin, L. & Bodis-Wollner, I. A combination of retinal morphology and visual electrophysiology testing increases diagnostic yield in Parkinson's disease. *Parkinsonism Relat. Disord.* **22** (Suppl. 1), S134–S137 (2016).
224. Zhang, J. R. et al. Correlations between retinal nerve fiber layer thickness and cognitive progression in Parkinson's disease: a longitudinal study. *Parkinsonism Relat. Disord.* **82**, 92–97 (2021).
225. Savy, C., Simon, A. & Nguyen-Legros, J. Spatial geometry of the dopamine innervation in the avascular area of the human fovea. *Vis. Neurosci.* **7**, 487–498 (1991).
226. Djamgoz, M. B., Hankins, M. W., Hirano, J. & Archer, S. N. Neurobiology of retinal dopamine in relation to degenerative states of the tissue. *Vis. Res.* **37**, 3509–3529 (1997).
227. Nir, I. & Iuvone, P. M. Alterations in light-evoked dopamine metabolism in dystrophic retinas of mutant rds mice. *Brain Res.* **649**, 85–94 (1994).
228. Miri, S. et al. The avascular zone and neuronal remodeling of the fovea in Parkinson disease. *Ann. Clin. Transl. Neurol.* **2**, 196–201 (2015).
229. Curcio, C. A. & Allen, K. A. Topography of ganglion cells in human retina. *J. Comp. Neurol.* **300**, 5–25 (1990).
230. Lee, J. Y., Ahn, J., Shin, J. Y. & Jeon, B. Parafoveal change and dopamine loss in the retina with Parkinson's disease. *Ann. Neurol.* **89**, 421–422 (2021).
231. Faucheux, B. A., Bonnet, A. M., Agid, Y. & Hirsch, E. C. Blood vessels change in the mesencephalon of patients with Parkinson's disease. *Lancet* **353**, 981–982 (1999).
232. Froger, N. et al. VEGF is an autocrine/paracrine neuroprotective factor for injured retinal ganglion neurons. *Sci. Rep.* **10**, 12409 (2020).
233. Desai Bradaric, B., Patel, A., Schneider, J. A., Carvey, P. M. & Hendey, B. Evidence for angiogenesis in Parkinson's disease, incidental Lewy body disease, and progressive supranuclear palsy. *J. Neural Transm.* **119**, 59–71 (2012).
234. Wada, K. et al. Expression levels of vascular endothelial growth factor and its receptors in Parkinson's disease. *Neuroreport* **17**, 705–709 (2006).
235. Yasuda, T. et al. Correlation between levels of pigment epithelium-derived factor and vascular endothelial growth factor in the striatum of patients with Parkinson's disease. *Exp. Neurol.* **206**, 308–317 (2007).
236. Lee, J. Y. et al. Lateral geniculate atrophy in Parkinson's with visual hallucination: a trans-synaptic degeneration? *Mov. Disord.* **31**, 547–554 (2016).
237. Oxtoby, N. P. et al. Sequence of clinical and neurodegeneration events in Parkinson's disease progression. *Brain* **144**, 975–988 (2021).
238. Williams-Gray, C. H., Foltynie, T., Brayne, C. E., Robbins, T. W. & Barker, R. A. Evolution of cognitive dysfunction in an incident Parkinson's disease cohort. *Brain* **130**, 1787–1798 (2007).
239. Zarkali, A., McColgan, P., Leyland, L. A., Lees, A. J. & Weil, R. S. Visual dysfunction predicts cognitive impairment and white matter degeneration in Parkinson's disease. *Mov. Disord.* **36**, 1191–1202 (2021).
240. Leyland, L. A. et al. Visual tests predict dementia risk in Parkinson disease. *Neurol. Clin. Pract.* **10**, 29–39 (2020).
241. Hong, S. B. et al. Contrast sensitivity impairment in drug-naive Parkinson's disease patients associates with early cognitive decline. *Neurol. Sci.* **41**, 1837–1842 (2020).
242. Akyol, E., Hagag, A. M., Sivaprasad, S. & Lotery, A. J. Adaptive optics: principles and applications in ophthalmology. *Eye* **35**, 244–264 (2021).
243. Dong, Z. M., Wollstein, G., Wang, B. & Schuman, J. S. Adaptive optics optical coherence tomography in glaucoma. *Prog. Retin. Eye Res.* **57**, 76–88 (2017).
244. Robbins, C. B. et al. Characterization of retinal microvascular and choroidal structural changes in Parkinson disease. *JAMA Ophthalmol.* **139**, 182–188 (2021).
245. Zou, J. et al. Combination of optical coherence tomography (OCT) and OCT angiography increases diagnostic efficacy of Parkinson's disease. *Quant. Imaging Med. Surg.* **10**, 1930–1939 (2020).
246. Koronyo, Y. et al. Retinal amyloid pathology and proof-of-concept imaging trial in Alzheimer's disease. *JCI Insight* **2**, e93621 (2017).
247. Yap, T. E., Donna, P., Almonte, M. T. & Cordeiro, M. F. Real-time imaging of retinal ganglion cell apoptosis. *Cells* **7**, 60 (2018).
248. Cordeiro, M. F. et al. Real-time imaging of single nerve cell apoptosis in retinal neurodegeneration. *Proc. Natl Acad. Sci. USA* **101**, 13352–13356 (2004).
249. Cordeiro, M. F. et al. Real-time imaging of single neuronal cell apoptosis in patients with glaucoma. *Brain* **140**, 1757–1767 (2017).

Author contributions

J.-Y.L., A.M.-B., A.M.-G. and N.C. researched data for the article. J.-Y.L., I.G., P.P. and B.J. contributed substantially to discussion of the content. J.-Y.L., A.M.-B., A.M.-G., I.G. and N.C. wrote the article. All authors reviewed and/or edited the manuscript before submission.

Competing interests

The authors declare no competing interests.

Peer review information

Nature Reviews Neurology thanks Y. Compta and the other, anonymous, reviewer(s) for their contribution to the peer review of this work.

Publisher's note

Springer Nature remains neutral with regard to jurisdictional claims in published maps and institutional affiliations.

Supplementary information

The online version contains supplementary material available at https://doi.org/10.1038/s41582-022-00618-9.